



**HAL**  
open science

## A Review of Innovation-Based Methods to Jointly Estimate Model and Observation Error Covariance Matrices in Ensemble Data Assimilation

Pierre Tandeo, Pierre Ailliot, Marc Bocquet, Alberto Carrassi, Takemasa Miyoshi, Manuel Pulido, Yicun Zhen

► **To cite this version:**

Pierre Tandeo, Pierre Ailliot, Marc Bocquet, Alberto Carrassi, Takemasa Miyoshi, et al.. A Review of Innovation-Based Methods to Jointly Estimate Model and Observation Error Covariance Matrices in Ensemble Data Assimilation. *Monthly Weather Review*, 2020, 148 (10), pp.3973-3994. 10.1175/MWR-D-19-0240.1 . hal-02922301

**HAL Id: hal-02922301**

<https://imt-atlantique.hal.science/hal-02922301v1>

Submitted on 26 Aug 2020

**HAL** is a multi-disciplinary open access archive for the deposit and dissemination of scientific research documents, whether they are published or not. The documents may come from teaching and research institutions in France or abroad, or from public or private research centers.

L'archive ouverte pluridisciplinaire **HAL**, est destinée au dépôt et à la diffusion de documents scientifiques de niveau recherche, publiés ou non, émanant des établissements d'enseignement et de recherche français ou étrangers, des laboratoires publics ou privés.



1 **A Review of Innovation-Based Methods to Jointly Estimate Model and**  
2 **Observation Error Covariance Matrices in Ensemble Data Assimilation**

3 Pierre Tandeo\*

4 *IMT Atlantique, Lab-STICC, UMR CNRS 6285, F-29238, France & RIKEN Center for*  
5 *Computational Science, Kobe, Japan*

6 Pierre Ailliot

7 *LMBA, UMR CNRS 6205, University of Brest, France*

8 Marc Bocquet

9 *CEREA Joint Laboratory École des Ponts ParisTech and EDF R&D, Université Paris-Est,*  
10 *Champs-sur-Marne, France*

11 Alberto Carrassi

12 *Dept. of Meteorology and National Centre for Earth Observation, University of Reading, UK &*  
13 *Mathematical Institute, University of Utrecht, Netherlands*

14 Takemasa Miyoshi

15 *RIKEN Center for Computational Science, Kobe, Japan*

16 Manuel Pulido

17 *Universidad Nacional del Nordeste and CONICET, Corrientes, Argentina & Department of*  
18 *Meteorology, University of Reading, UK*

19 Yicun Zhen

20 *IMT Atlantique, Lab-STICC, UMR CNRS 6285, F-29238, France*

21 *\*Corresponding author address: Dept. Signal & Communications, IMT Atlantique, 655 Avenue*  
22 *du Technopôle, 29200 Plouzané, France*  
23 *E-mail: pierre.tandeo@imt-atlantique.fr*

## ABSTRACT

24 Data assimilation combines forecasts from a numerical model with observa-  
25 tions. Most of the current data assimilation algorithms consider the model and  
26 observation error terms as additive Gaussian noise, specified by their covari-  
27 ance matrices  $Q$  and  $R$ , respectively. These error covariances, and specifically  
28 their respective amplitudes, determine the weights given to the background  
29 (i.e., the model forecasts) and to the observations in the solution of data as-  
30 simulation algorithms (i.e., the analysis). Consequently,  $Q$  and  $R$  matrices sig-  
31 nificantly impact the accuracy of the analysis. This review aims to present and  
32 to discuss, with a unified framework, different methods to jointly estimate the  
33  $Q$  and  $R$  matrices using ensemble-based data assimilation techniques. Most  
34 of the methodologies developed to date use the innovations, defined as differ-  
35 ences between the observations and the projection of the forecasts onto the  
36 observation space. These methodologies are based on two main statistical  
37 criteria: (i) the method of moments, in which the theoretical and empirical  
38 moments of the innovations are assumed to be equal, and (ii) methods that  
39 use the likelihood of the observations, themselves contained in the innova-  
40 tions. The reviewed methods assume that innovations are Gaussian random  
41 variables, although extension to other distributions is possible for likelihood-  
42 based methods. The methods also show some differences in terms of levels of  
43 complexity and applicability to high-dimensional systems. The conclusion of  
44 the review discusses the key challenges to further develop estimation meth-  
45 ods for  $Q$  and  $R$ . These challenges include taking into account time-varying  
46 error covariances, using limited observational coverage, estimating additional  
47 deterministic error terms, or accounting for correlated noise.

## 48 1. Introduction

49 In meteorology and other environmental sciences, an important challenge is to estimate the state  
50 of the system as accurately as possible. In meteorology, this state includes pressure, humidity,  
51 temperature and wind at different locations and elevations in the atmosphere. Data assimilation  
52 (hereinafter DA) refers to mathematical methods that use both model predictions (also called back-  
53 ground information) and partial observations to retrieve the current state vector with its associated  
54 error. An accurate estimate of the current state is crucial to get good forecasts, and it is particularly  
55 so whenever the system dynamics is chaotic, such as it is the case for the atmosphere.

56 The performance of a DA system to estimate the state depends on the accuracy of the model  
57 predictions, the observations, and their associated error terms. A simple, popular and mathemat-  
58 ically justifiable way of modeling these errors is to assume them to be independent and unbiased  
59 Gaussian white noise, with covariance matrices  $\mathbf{Q}$  for the model and  $\mathbf{R}$  for the observations. Given  
60 the aforementioned importance of  $\mathbf{Q}$  and  $\mathbf{R}$  in estimating the analysis state and error, a number of  
61 studies dealing with this problem has arisen in the last decades. This review work presents and  
62 summarizes the different techniques used to estimate simultaneously the  $\mathbf{Q}$  and  $\mathbf{R}$  covariances.  
63 Before discussing the methods to achieve this goal, the mathematical formulation of DA is briefly  
64 introduced.

### 65 *a. Problem statement*

66 Hereinafter, the unified DA notation proposed in Ide et al. (1997) is used<sup>1</sup>. DA algorithms are  
67 used to estimate the state of a system,  $\mathbf{x}$ , conditionally on observations,  $\mathbf{y}$ . A classic strategy is to  
68 use sequential and ensemble DA frameworks, as illustrated in Fig. 1, and to combine two sources  
69 of information: model forecasts (in green) and observations (in blue). The ensemble framework

---

<sup>1</sup>Other notations are also used in practice

70 uses different realizations, also called members, to track the state of the system at each assimilation  
71 time step.

72 The forecasts of the state are based on the usually incomplete and approximate knowledge of the  
73 system dynamics. The evolution of the state from time  $k - 1$  to  $k$  is given by the model equation:

$$\mathbf{x}(k) = \mathcal{M}_k(\mathbf{x}(k-1)) + \boldsymbol{\eta}(k), \quad (1)$$

74 where the model error  $\boldsymbol{\eta}$  implies that the dynamic model operator  $\mathcal{M}_k$  is not perfectly known.  
75 Model error is usually assumed to follow a Gaussian distribution with zero mean (i.e., the model  
76 is unbiased) and covariance  $\mathbf{Q}$ . The dynamic model operator  $\mathcal{M}_k$  in Eq. (1) has also an explicit  
77 dependence on  $k$ , because it may depend on time-dependent external forcing terms. At time  $k$ ,  
78 the forecasted state is characterized by the mean of the forecasted states,  $\mathbf{x}^f$ , and its uncertainty  
79 matrix, namely  $\mathbf{P}^f$ , which is also called the background error covariance matrix, and noted  $\mathbf{B}$  in  
80 DA.

81 The forecast covariance  $\mathbf{P}^f$  is determined by two processes. The first is the uncertainty propa-  
82 gated from  $k - 1$  to  $k$  by the model  $\mathcal{M}_k$  (the green shade within the dashed ellipse in Fig. 1, and  
83 denoted by  $\mathbf{P}^m$ ). The second process is the model error covariance  $\mathbf{Q}$  accounted by the noise term  
84 at time  $k$  in Eq. (1). Given that model error is largely unknown and originated by various and  
85 diverse sources, the matrix  $\mathbf{Q}$  is also poorly known. Model error sources encompass the model  $\mathcal{M}$   
86 deficiencies to represent the underlying physics, including deficiencies in the numerical schemes,  
87 the cumulative effects of errors in the parameters, and the lack of knowledge of the unresolved  
88 scales. Its estimation is a challenge in general, but it is particularly so in geosciences because we  
89 usually have far fewer observations than those needed to estimate the entries of  $\mathbf{Q}$  (Daley 1992;  
90 Dee 1995). The sum of the two covariances  $\mathbf{P}^m$  and  $\mathbf{Q}$  gives the forecast covariance matrix,  $\mathbf{P}^f$   
91 (full green ellipse in Fig. 1). In the illustration given here, a large contribution of the forecast co-

92 variance  $\mathbf{P}^f$  is due to  $\mathbf{Q}$ . This situation reflects what is common in ensemble DA, where  $\mathbf{P}^m$  can be  
 93 too small, as a consequence of the ensemble undersampling of the initial condition error (i.e., the  
 94 covariance estimated at the previous analysis). In that case, inflating  $\mathbf{Q}$  could partially compensate  
 95 for the bad specification of  $\mathbf{P}^m$ .

96 DA uses a second source of information, the observations  $\mathbf{y}$ , which are assumed to be linked to  
 97 the true state  $\mathbf{x}$  through the time-dependent operator  $\mathcal{H}_k$ . This step in DA algorithms is formalized  
 98 by the observation equation:

$$\mathbf{y}(k) = \mathcal{H}_k(\mathbf{x}(k)) + \boldsymbol{\epsilon}(k), \quad (2)$$

99 where the observation error  $\boldsymbol{\epsilon}$  describes the discrepancy between what is observed and the truth.  
 100 In practice, it is important to remove as much as possible the large-scale bias in the observation  
 101 before DA. Then, it is common to state that the remaining error  $\boldsymbol{\epsilon}$  follows a Gaussian and unbiased  
 102 distribution with a covariance  $\mathbf{R}$  (the blue ellipse in Fig. 1). This covariance takes into account er-  
 103 rors in the observation operator  $\mathcal{H}$ , the instrumental noise and the representation error associated  
 104 with the observation, typically measuring a higher resolution state than the model represents. Op-  
 105 erationally, a correct estimation of  $\mathbf{R}$  that takes into account all these effects is often challenging  
 106 (Janjić et al. 2018).

107 DA algorithms combine forecasts with observations, based on the model and observation equa-  
 108 tions, respectively given in Eq. (1) and Eq. (2). The corresponding system of equations is a non-  
 109 linear state-space model. As illustrated in Fig. 1, this Gaussian DA process produces a posterior  
 110 Gaussian distribution with mean  $\mathbf{x}^a$  and covariance  $\mathbf{P}^a$  (red ellipse). The system given in Eqs. (1)  
 111 and (2) is representative of a broad range of DA problems, as described in seminal papers such  
 112 as Ghil and Malanotte-Rizzoli (1991), and still relevant today as referenced by Houtekamer and  
 113 Zhang (2016) and Carrassi et al. (2018). The assumptions made in Eqs. (1) and (2) about model  
 114 and observation errors (additive, Gaussian, unbiased, and mutually independent) are strong, yet



115 convenient from the mathematical and computational point of view. Nevertheless, these assump-  
116 tions are not always realistic in real DA problems. For instance, in operational applications, sys-  
117 tematic biases in the model and in the observations are recurring problems. Indeed, biases affect  
118 significantly the DA estimations and a specific treatment is required; see Dee (2005) for more  
119 details.

120 From Eqs. (1) and (2), noting that  $\mathcal{M}$ ,  $\mathcal{H}$  and  $\mathbf{y}$  are given, the only parameters that influence the  
121 estimation of  $\mathbf{x}$  are the covariance matrices  $\mathbf{Q}$  and  $\mathbf{R}$ . These covariances play an important role in  
122 DA algorithms. Their importance was early put forward in Hollingsworth and Lönnberg (1986),  
123 in section 4.1 of Ghil and Malanotte-Rizzoli (1991) and Daley (1991) in section 4.9. The results  
124 of DA algorithms highly depend on the two error covariance matrices  $\mathbf{Q}$  and  $\mathbf{R}$ , which have to be  
125 specified by the users. But these covariances are not easy to tune. Indeed, their impact is hard to  
126 grasp in real DA problems with high-dimensionality and nonlinear dynamics. We thus illustrate  
127 the problem with a simple example first.

### 128 *b. Illustrative example*

129 In either variational or ensemble-based DA methods, the quality of the reconstructed state (or  
130 hidden) vector  $\mathbf{x}$  largely depends on the relative amplitudes between the assumed observation and  
131 model errors (Desroziers and Ivanov 2001). In Kalman filter based methods, the signal-to-noise  
132 ratio  $\|\mathbf{P}^f\| / \|\mathbf{R}\|$ , where  $\mathbf{P}^f$  depends on  $\mathbf{Q}$ , impacts the Kalman gain, which gives the relative  
133 weights of the observations against the model forecasts. Here, the  $\|\cdot\|$  operator represents a matrix  
134 norm. For instance, Berry and Sauer (2013) used the Frobenius norm to study the effect of this  
135 ratio in the reconstruction of the state in toy models.

136 The importance of  $\mathbf{Q}$ ,  $\mathbf{R}$  and  $\|\mathbf{P}^f\| / \|\mathbf{R}\|$  is illustrated with the aid of a toy example, using  
137 a scalar state  $x$  and simple linear dynamics. This simplified setup avoids several issues typical

138 of realistic DA applications: the large dimension of the state, the strong nonlinearities and the  
139 chaotic behavior. In this example, the dynamic model in Eq. (1) is a first-order autoregressive  
140 model, denoted by AR(1) and defined by

$$x(k) = 0.95x(k-1) + \eta(k), \quad (3)$$

141 with  $\eta \sim \mathcal{N}(0, Q^t)$  where the superscript  $t$  means “true” and  $Q^t = 1$ . Furthermore, observations  $y$   
142 of the state are contaminated with an independent additive zero-mean and unit-variance Gaussian  
143 noise, such that  $R^t = 1$  in Eq. (2) with  $\mathcal{H}(x) = x$ . The goal is to reconstruct  $x$  from the noisy ob-  
144 servations  $y$  at each time step. The AR(1) dynamic model defined by Eq. (3) has an autoregressive  
145 coefficient close to one, representing a process which evolves slowly over time, and a stochastic  
146 noise term  $\eta$  with variance  $Q^t$ . Although the knowledge of these two sources of noise is crucial  
147 for the estimation problem, identifying them is not an easy task. Given that the dynamic model is  
148 linear and the error terms are additive and Gaussian in this simple example, the Kalman smoother  
149 provides the best estimation of the state (see section 2 for more details). To evaluate the effect  
150 of badly specified  $Q$  and  $R$  errors on the reconstructed state with the Kalman smoother, different  
151 experiments were conducted with values of  $\{0.1, 1, 10\}$  for the ratio  $Q/R$  (in this toy example, we  
152 use  $Q/R$  instead of  $\|\mathbf{P}^f\| / \|\mathbf{R}\|$  for simplicity).

153 Figure 2 shows, as a function of time, the true state (red line) and the smoothing Gaussian  
154 distributions represented by the 95% confidence intervals (gray shaded) and their means (black  
155 lines). We also report the Root Mean Squared Error (RMSE) of the reconstruction and the so-  
156 called “coverage probability”, or percentage of  $x$  that falls in the 95% confidence intervals (defined  
157 as the mean  $\pm 1.96$  the standard deviation in the Gaussian case). In this synthetic experiment, the  
158 best RMSE and coverage probability obtained, applying the Kalman smoother with true  $Q^t =$   
159  $R^t = 1$ , are 0.71 and 95%, respectively. Using a small model error variance  $Q = 0.1Q^t$  in Fig. 2(a),

160 the filter gives a large weight to the forecasts given by the quasi-persistent autoregressive dynamic  
161 model. On the other hand, with a small observation error variance  $R = 0.1R'$  in Fig. 2(b), excessive  
162 weight is given to the observation and the reconstructed state is close to the noisy measurements.  
163 These results show the negative impact of independently badly scaled  $Q$  and  $R$  error variances. In  
164 the case of overestimated model error variance as in Fig. 2(c), the mean reconstructed state vector  
165 and thus its RMSE are identical to Fig. 2(b). In the same way, overestimated observation error  
166 variance like in Fig. 2(d) gives similar mean reconstruction, as in Fig. 2(a). These last two results  
167 are due to the fact that in both cases, the ratio  $Q/R$  are equal, respectively, to 10 and 0.1. Now,  
168 we consider in Fig. 2(e) and Fig. 2(f) the case where the  $Q/R$  ratio is equal to 1, but, respectively,  
169 using the simultaneous underestimation and overestimation of model and observation errors. In  
170 both cases, the mean reconstructed state is equal to that obtained with the true error variances (i.e.,  
171 RMSE=0.71). The main difference is the gray confidence interval, which is supposed to contain  
172 95% of the true trajectory: the spread is clearly underestimated in Fig. 2(e) and overestimated in  
173 Fig. 2(f), with respective coverage probability of 36% and 100%.

174 We used a simple synthetic example, but for large dimensional and highly nonlinear dynamics,  
175 such an underestimation or overestimation of uncertainty may have a strong effect and may cause  
176 filters to collapse. The main issue in ensemble-based DA is an underdispersive spread, as in  
177 Fig. 2(e). In that case, the initial condition spread is too narrow, and model forecasts (starting  
178 from these conditions) would be similar and potentially out of the range of the observations. In  
179 the case of an overdispersive spread, as in Fig. 2(f), the risk is that only a small portion of model  
180 forecasts would be accurate enough to produce useful information on the true state of the system.  
181 This illustrative example shows how important is the joint tuning of model and observation errors  
182 in DA. Since the 1990s, a substantial number of studies have dealt with this topic.

183 *c. Seminal work in the data assimilation community*

184 In a seminal paper, Dee (1995) proposed an estimation method for parametric versions of  $\mathbf{Q}$   
185 and  $\mathbf{R}$  matrices. The method, based on maximizing the likelihood of the observations, yields an  
186 estimator which is a function of the innovation defined by  $\mathbf{y} - \mathcal{H}(\mathbf{x}^f)$ . Maximization is performed  
187 at each assimilation step, with the current innovation computed from the available observations.  
188 This technique was later extended to estimate the mean of the innovation, which depends on the  
189 biases in the forecast and in the observations (Dee et al. 1999a). The methodology was then  
190 applied to realistic cases in Dee et al. (1999b), making the maximization of innovation likelihood  
191 a promising technique for the estimation of errors in operational forecasts.

192 Following a distinct path, Desroziers and Ivanov (2001) proposed using the observation-minus-  
193 analysis diagnostic. It is defined by  $\mathbf{y} - \mathcal{H}(\mathbf{x}^a)$  with  $\mathbf{x}^a$  the analysis (i.e., the output of DA algo-  
194 rithms). The authors proposed an iterative optimization technique to estimate a scaling factor for  
195 the background  $\mathbf{B} = \mathbf{P}^f$  and observation  $\mathbf{R}$  matrices. The procedure was shown to converge to a  
196 proper fixed-point. As in Dee's work, the fixed-point method presented in Desroziers and Ivanov  
197 (2001) is applied at each assimilation step, with the available observations at the current step.

198 Later, Chapnik et al. (2004) showed that the maximization of the innovation likelihood proposed  
199 by Dee (1995) makes the observation-minus-analysis diagnostic of Desroziers and Ivanov (2001)  
200 optimal. Moreover, the techniques of Dee (1995) and Desroziers and Ivanov (2001) have been  
201 further connected to the generalized cross-validation method previously developed by statisticians  
202 (Wahba and Wendelberger 1980).

203 These initial studies clearly nurtured the discussion of the estimation of observation  $\mathbf{R}$ , model  $\mathbf{Q}$ ,  
204 or background  $\mathbf{B} = \mathbf{P}^f$  error covariance matrices in the modern DA literature. For demonstration  
205 purposes, the algorithms proposed in Dee (1995) and Desroziers and Ivanov (2001) were tested on

206 realistic DA problems, using a shallow-water model on a plane with a simplified Kalman filter, and  
207 using the French ARPEGE three-dimensional variational framework, respectively. In both cases,  
208 although good performances have been obtained with a small number of iterations, the proposed  
209 algorithms have shown some limits, in particular with regard to the simultaneous estimation of the  
210 two sources of errors: observation and model (or background). In this context, Todling (2015)  
211 pointed out that using only the current innovation is not enough to distinguish the impact of  $\mathbf{Q}$  and  
212  $\mathbf{R}$ , which still makes their simultaneous estimation challenging. Given that our preliminary focus  
213 here is to review methods for the joint estimate of  $\mathbf{Q}$  and  $\mathbf{R}$ , the work Dee (1995) and Desroziers  
214 and Ivanov (2001) are not further detailed hereafter. After these two seminal studies, various  
215 alternatives were proposed. They are based on the use of several types of innovations and are  
216 discussed in this review.

#### 217 *d. Methods presented in this review*

218 The main topic of this review is the “joint estimation of  $\mathbf{Q}$  and  $\mathbf{R}$ ”. Thus, only methods based  
219 on this specific goal are presented in detail. A history of what have been, in our opinion, the most  
220 relevant contributions and the key milestones for  $\mathbf{Q}$  and  $\mathbf{R}$  covariance estimation in DA is sketched  
221 in Fig. 3. The highlighted papers are discussed in this review, with a summary of the different  
222 methodologies, given in Table 1. We distinguish four methods and we can classify them into  
223 two categories: those which rely on moment-based methods, and those using likelihood-based  
224 methods. Both methods make use of the innovations. The main concepts of the techniques are  
225 briefly introduced below.

226 On the one hand, moment-based methods assume equality between theoretical and empirical  
227 statistical moments. A first approach is to study different type of innovations in the observation  
228 space (i.e., working in the space of the observations instead of the space of the state). It has

229 been initiated in DA by Rutherford (1972) and Hollingsworth and Lönnberg (1986). A second  
230 approach extracts information from the correlation between lag innovations, namely innovations  
231 between consecutive times. On the other hand, likelihood-based methods aim to maximize likeli-  
232 hood functions with statistical algorithms. One option is to use a Bayesian framework, assuming  
233 prior distributions for the parameters of  $\mathbf{Q}$  and  $\mathbf{R}$  covariance matrices. Another option is to use the  
234 iterative expectation–maximization algorithm to maximize a likelihood function.

235 The four methodologies listed in Fig. 3 will be examined in this paper. Before doing that, it is  
236 worth mentioning existing review work that have attempted to summarize the methodologies in  
237 DA context and beyond.

#### 238 *e. Other review papers*

239 Other review papers on parameter estimation (including  $\mathbf{Q}$  and  $\mathbf{R}$  matrices) in state-space models  
240 have appeared in the statistical and signal processing communities. The first one (Mehra 1972)  
241 introduces moment- and likelihood-based methods in the linear and Gaussian case (i.e., when  $\boldsymbol{\eta}$   
242 and  $\boldsymbol{\epsilon}$  are Gaussians and  $\mathcal{M}$  is a linear operator in Eqs. (1) and (2)). Many extensions to nonlinear  
243 state-space models have been proposed since the seminal work of Mehra, and these studies are  
244 summarized in the recent review by Duník et al. (2017), with a focus on moment-based methods  
245 and the extended Kalman filter (Jazwinski 1970). The book chapter by Buehner (2010) presents  
246 another review of moment-based methods, with a focus on the modeling and estimation of spatial  
247 covariance structures  $\mathbf{Q}$  and  $\mathbf{R}$  in DA with the ensemble Kalman filter algorithm (Evensen 2009).

248 In the statistical community, the recent development of powerful simulation techniques, known  
249 as sequential Monte-Carlo algorithms or particle filters, has led to an extensive literature on the  
250 statistical inference in nonlinear state-space models relying on likelihood-based approaches. A  
251 recent and detailed presentation of this literature can be found in Kantas et al. (2015). However,

252 these methods typically require a large number of particles, which make them impractical for  
253 geophysical DA applications.

254 The review presented here focuses on methods proposed in DA, especially the moment- and  
255 likelihood-based techniques which are suitable for geophysical systems (i.e., with high dimen-  
256 sionality and strong nonlinearities).

#### 257 *f. Structure of this review*

258 The paper is organized as follows. Section 2 briefly presents the filtering and smoothing DA  
259 algorithms used in this work. The main families of methods used in the literature to jointly  
260 estimate error covariance matrices  $\mathbf{Q}$  and  $\mathbf{R}$  are then described. First, moment-based methods  
261 are introduced in section 3. Then, we describe in section 4 the likelihood-based methods. We  
262 also mention other alternatives in section 5, along with methods used in the past but not exactly  
263 matching the scope of this review, and diagnostic tools to check the accuracy of  $\mathbf{Q}$  and  $\mathbf{R}$ . Finally,  
264 in section 6, we provide a summary and discussion on what we consider to be the forthcoming  
265 challenges in this area.

## 267 **2. Filtering and smoothing algorithms**

268 This review paper focuses on the estimation of  $\mathbf{Q}$  and  $\mathbf{R}$  in the context of ensemble-based DA  
269 methods. For the overall discussion of the methods and to set the notation, a short description of  
270 the ensemble version of the Kalman recursions is presented in this section: the ensemble Kalman  
271 filter (EnKF) and ensemble Kalman smoother (EnKS).

272 The EnKF and EnKS estimate various state vectors  $\mathbf{x}^f(k)$ ,  $\mathbf{x}^a(k)$ ,  $\mathbf{x}^s(k)$  and covariance matrices  
273  $\mathbf{P}^f(k)$ ,  $\mathbf{P}^a(k)$ ,  $\mathbf{P}^s(k)$ , at each time step  $1 \leq k \leq K$ , where  $K$  represents the total number of assimila-

274 tion steps. Kalman-based algorithms assume a Gaussian prior distribution  $p(\mathbf{x}(k)|\mathbf{y}(1:k-1)) \sim$   
275  $\mathcal{N}(\mathbf{x}^f(k), \mathbf{P}^f(k))$ . Then, filtering and smoothing estimates correspond to the Gaussian posterior  
276 distributions  $p(\mathbf{x}(k)|\mathbf{y}(1:k)) \sim \mathcal{N}(\mathbf{x}^a(k), \mathbf{P}^a(k))$  and  $p(\mathbf{x}(k)|\mathbf{y}(1:K)) \sim \mathcal{N}(\mathbf{x}^s(k), \mathbf{P}^s(k))$  of the  
277 state conditionally to past/present observations and past/present/future observations respectively.

278 The basic idea of the EnKF and EnKS is to use an ensemble  $\mathbf{x}_1, \dots, \mathbf{x}_{N_e}$  of size  $N_e$  to track  
279 Gaussian distributions over time with the empirical mean vector  $\bar{\mathbf{x}} = 1/N_e \sum_{i=1}^{N_e} \mathbf{x}_i$  and the empirical  
280 error covariance matrix  $1/(N_e-1) \sum_{i=1}^{N_e} (\mathbf{x}_i - \bar{\mathbf{x}})(\mathbf{x}_i - \bar{\mathbf{x}})^T$ .



The EnKF/EnKS equations are divided into three main steps,  $\forall i = 1, \dots, N_e$  and  $\forall k = 1, \dots, K$ :

Forecast step (forward in time):

$$\mathbf{x}_i^f(k) = \mathcal{M}_k(\mathbf{x}_i^a(k-1)) + \boldsymbol{\eta}_i(k) \quad (4a)$$

Analysis step (forward in time):

$$\mathbf{d}_i(k) = \mathbf{y}(k) - \mathcal{H}_k(\mathbf{x}_i^f(k)) + \boldsymbol{\varepsilon}_i(k) \quad (4b)$$

$$\mathbf{K}^f(k) = \mathbf{P}^f(k) \mathcal{H}_k^\top \left( \mathcal{H}_k \mathbf{P}^f(k) \mathcal{H}_k^\top + \mathbf{R}(k) \right)^{-1} \quad (4c)$$

$$\mathbf{x}_i^a(k) = \mathbf{x}_i^f(k) + \mathbf{K}^f(k) \mathbf{d}_i(k) \quad (4d)$$

Reanalysis step (backward in time):

$$\mathbf{K}^s(k) = \mathbf{P}^a(k) \mathcal{M}_k^\top \left( \mathbf{P}^f(k+1) \right)^{-1} \quad (4e)$$

$$\mathbf{x}_i^s(k) = \mathbf{x}_i^a(k) + \mathbf{K}^s(k) \left( \mathbf{x}_i^s(k+1) - \mathbf{x}_i^f(k+1) \right) \quad (4f)$$

282 with  $\mathbf{K}^f(k)$  and  $\mathbf{K}^s(k)$  the filter and smoother Kalman gains, respectively. Here,  $\mathbf{P}^f(k)$  and  
 283  $\mathcal{H}_k \mathbf{P}^f(k) \mathcal{H}_k^\top$  denote the empirical covariance matrices of  $\mathbf{x}_i^f(k)$  and  $\mathcal{H}_k(\mathbf{x}_i^f(k))$ , respectively.  
 284 Then,  $\mathbf{P}^f(k) \mathcal{H}_k^\top$  and  $\mathbf{P}^a(k) \mathcal{M}_k^\top$  denote the empirical cross-covariance matrices between  $\mathbf{x}_i^f(k)$   
 285 and  $\mathcal{H}_k(\mathbf{x}_i^f(k))$  and between  $\mathbf{x}_i^a(k)$  and  $\mathcal{M}_k(\mathbf{x}_i^a(k))$ , respectively. These quantities are estimated  
 286 using  $N_e$  ensemble members.

287 In some of the methods presented in this review, the ensembles are also used to approximate  $\mathcal{M}_k$   
 288 and  $\mathcal{H}_k$  by linear operators  $\mathbf{M}_k$  and  $\mathbf{H}_k$  such as

$$\mathbf{M}_k = \mathbf{E}_k^{\mathcal{M}(a)} (\mathbf{E}_{k-1}^a)^\dagger \quad (5a)$$

$$\mathbf{H}_k = \mathbf{E}_k^{\mathcal{H}(f)} (\mathbf{E}_k^f)^\dagger \quad (5b)$$

289 with  $\dagger$  the pseudo-inverse,  $\mathbf{E}_k^{\mathcal{M}(a)}$ ,  $\mathbf{E}_{k-1}^a$ ,  $\mathbf{E}_k^{\mathcal{H}(f)}$  and  $\mathbf{E}_k^f$  the matrices containing along their  
290 columns the ensemble perturbation vectors (the centered ensemble vectors) of  $\mathcal{M}_k(\mathbf{x}_i^a(k-1))$ ,  
291  $\mathbf{x}_i^a(k-1)$ ,  $\mathcal{H}_k(\mathbf{x}_i^f(k))$  and  $\mathbf{x}_i^f(k)$ , respectively.

292 In Eq. (4b), the innovation is denoted as  $\mathbf{d}$  and tracked by  $\mathbf{d}_1(k), \dots, \mathbf{d}_{N_e}(k)$ . The innovation is  
293 the key ingredient of the methods presented in sections 3 and 4.

### 294 3. Moment-based methods

295 In order to constrain the model and observational errors in DA systems, initial efforts were fo-  
296 cused on the statistics of relevant variables which could contain information on covariances. The  
297 innovation, given in Eq. (4b), corresponds to the difference between the observations and the fore-  
298 cast in the observation space. This variable implicitly takes into account the  $\mathbf{Q}$  and  $\mathbf{R}$  covariances.  
299 Unfortunately, as explained in Blanchet et al. (1997), by using only current observations, their  
300 individual contributions cannot be easily disentangled. Thus, the techniques with only the classic  
301 innovation  $\mathbf{y}(k) - \mathcal{H}_k(\mathbf{x}^f(k))$  are not discussed further in this review.

302 Two main approaches have been proposed in the literature to address this issue. They are based  
303 on the idea of producing multiple equations involving  $\mathbf{Q}$  and  $\mathbf{R}$ . The first approach uses different  
304 type of innovation statistics (i.e., not only the classic one). The second approach is based on lag  
305 innovations, or differences between consecutive innovations. From a statistical point of view, they  
306 refer to the “methods of moments”, where we construct a system of equations that links various  
307 moments of the innovations with the parameters and then replace the theoretical moments by the  
308 empirical ones in these equations.

309 *a. Innovation statistics in the observation space*

310 This first approach, based on the Desroziers diagnostic (Desroziers et al. 2005), is historical  
 311 and now popular in the DA community. It does not exactly fit the topic of this review paper (i.e.,  
 312 estimating the model error  $\mathbf{Q}$ ), since it is based on the inflation of the background covariance  
 313 matrix  $\mathbf{P}^f$ . However, this forecast error covariance is defined by  $\mathbf{P}^f(k) = \mathbf{M}_k \mathbf{P}^a(k-1) \mathbf{M}_k^T + \mathbf{Q}$  in  
 314 the Kalman filter, considering a linear model operator  $\mathbf{M}_k$ . Thus, even if DA systems do not use  
 315 an explicit model error perturbation controlled by  $\mathbf{Q}$ , the inflation of the background covariance  
 316 matrix  $\mathbf{P}^f$  has similar effects, compensating for the lack of an explicit model uncertainty.

Desroziers et al. (2005) proposed examining various innovation statistics in the observation space. It is based on different type of innovation statistics between observations, forecasts and analysis, with all of them defined in the observation space: namely,  $\mathbf{d}^{o-f}(k) = \mathbf{y}(k) - \mathcal{H}_k(\mathbf{x}^f(k))$  as in Eq. (4b) and  $\mathbf{d}^{o-a}(k) = \mathbf{y}(k) - \mathcal{H}_k(\mathbf{x}^a(k))$ . In theory, in the linear and Gaussian case, for unbiased forecast and observation, and when  $\mathbf{P}^f(k)$  and  $\mathbf{R}(k)$  are correctly specified, the Desroziers innovation statistics should verify the equalities:

$$\begin{cases} \mathbb{E} \left[ \mathbf{d}^{o-f}(k) \mathbf{d}^{o-f}(k)^T \right] = \mathbf{H}_k \mathbf{P}^f(k) \mathbf{H}_k^T + \mathbf{R}(k) & (6a) \\ \mathbb{E} \left[ \mathbf{d}^{o-a}(k) \mathbf{d}^{o-f}(k)^T \right] = \mathbf{R}(k) & (6b) \end{cases}$$

317 with E the expectation operator. Equation (6a) is given by using Eq. (4b):

$$\begin{aligned} \mathbf{d}^{o-f}(k) \mathbf{d}^{o-f}(k)^T &= -\mathbf{y}(k) \mathbf{x}^f(k)^T \mathbf{H}_k^T \\ &\quad - \mathbf{H}_k \mathbf{x}^f(k) \mathbf{y}(k)^T \\ &\quad + \mathbf{H}_k \mathbf{x}^f(k) \mathbf{x}^f(k)^T \mathbf{H}_k^T \\ &\quad + \mathbf{y}(k) \mathbf{y}(k)^T, \end{aligned} \quad (7)$$

318 then applying the expectation operator and using the definition of  $\mathbf{P}^f$  and  $\mathbf{R}$ . The observation-  
 319 minus-forecast innovation statistics in Eq. (6a) is not useful to constrain model error  $\mathbf{Q}$ . Indeed,

320  $\mathbf{d}^{o-f}$  does not depend explicitly on  $\mathbf{Q}$ , but rather on the forecast error covariance matrix  $\mathbf{P}^f$ . Thus,  
321 the combination of Eq. (6a) and Eq. (6b) can be used as a diagnosis of the forecast and obser-  
322 vational error covariances in the system. A mismatch between the Desroziers statistics and the  
323 actual covariances, namely the left- and right-hand side terms in Eq. (6a) and Eq. (6b), indicates  
324 inappropriate estimated covariances  $\mathbf{P}^f(k)$  and  $\mathbf{R}(k)$ .

325 The forecast covariance  $\mathbf{P}^f$  is sometimes badly estimated in ensemble-based assimilation sys-  
326 tems. The limitations may be attributed to a number of causes. The limited number of ensemble  
327 members produces an over- or, most of the time, underestimation of the forecast variance. An-  
328 other limitation is the inaccuracies in methods used to sample initial condition or model error. The  
329 underestimation of the forecast covariance produces negative feedback, and the estimated analysis  
330 covariance  $\mathbf{P}^a$  is thus underestimated, which in turn produces a further underestimation of the fore-  
331 cast covariance in the next cycle. This feedback process leads to filter divergence, as was pointed  
332 out by Pham et al. (1998), Anderson and Anderson (1999) or Anderson (2007). To avoid this  
333 filter divergence, inflating the forecast covariance  $\mathbf{P}^f$  has been proposed. This covariance inflation  
334 accounts for both sampling errors and the lack of representation of model errors, like a too small  
335 amplitude for  $\mathbf{Q}$  or the fact that a bias is omitted in  $\boldsymbol{\eta}$  and  $\boldsymbol{\epsilon}$ , Eqs. (1) and (2). In this context, the  
336 diagnostics given by the Desroziers innovation statistics have been proposed as a tool to constrain  
337 the required covariance inflation in the system.

338 We distinguish three inflation methods: multiplicative, additive and relaxation-to-prior. In the  
339 multiplicative case, the forecast error covariance matrix  $\mathbf{P}^f$  is usually multiplied by a scalar coeffi-  
340 cient greater than 1 (Anderson and Anderson 1999). Using innovation statistics in the observation  
341 space, adaptive procedures to estimate this coefficient have been proposed by Wang and Bishop  
342 (2003), Anderson (2007), Anderson (2009) conditionally to the spatial location, Li et al. (2009),  
343 Miyoshi (2011), Bocquet (2011), Bocquet and Sakov (2012), Miyoshi et al. (2013), Bocquet et al.

344 (2015), El Gharamti (2018) and Raanes et al. (2019). In order to prevent excessive inflation or de-  
345 flation, some authors have proposed assuming a priori distribution for the multiplicative inflation  
346 factor. The most usual a priori distributions used by the authors are Gaussian in Anderson (2009),  
347 inverse-gamma in El Gharamti (2018) or inverse chi-square in Raanes et al. (2019).

348 In practice, multiplicative inflation tends to excessively inflate in the data-sparse regions and  
349 inflate too little in the densely observed regions. As a result, the spread looks like exaggeration of  
350 data density (i.e., too much spread in sparsely observed regions, and vice versa). Additive inflation  
351 solves this problem, but requires a lot of samples for additive noise; these drawbacks and benefits  
352 are discussed in Miyoshi et al. (2010). In the additive inflation case, the diagonal terms of the  
353 forecast and analysis empirical covariance matrices is increased (Mitchell and Houtekamer 2000;  
354 Corazza et al. 2003; Whitaker et al. 2008; Houtekamer et al. 2009). This regularization also avoids  
355 the problems corresponding to the inversion of the covariance matrices.

356 The last alternative is the relaxation-to-prior method. In application, this technique is more effi-  
357 cient than both additive and multiplicative inflations because it maintains a reasonable spread struc-  
358 ture. The idea is to relax the reduction of the spread at analysis. We distinguish the method pro-  
359 posed in Zhang et al. (2004), where the forecast and analysis ensemble perturbations are blended,  
360 from the one given in Whitaker and Hamill (2012), which multiplies the analysis ensemble with-  
361 out blending perturbations. This last method is thus a multiplicative inflation, but applied after the  
362 analysis, not the forecast. Finally, Ying and Zhang (2015) and Kotsuki et al. (2017b) proposed  
363 methods to adaptively estimate the relaxation parameters using innovation statistics. Their con-  
364 clusions are that adaptive procedures for relaxation-to-prior methods are robust to sudden changes  
365 in the observing networks and observation error settings.

366 Closely connected to multiplicative inflation estimation is statistical modeling of the error vari-  
367 ance terms proposed by Bishop and Satterfield (2013) and Bishop et al. (2013). From numerical

368 evidence based on the 10-dimensional Lorenz-96 model, the authors assume an inverse-gamma  
 369 prior distribution for these variances. This distribution allows for an analytic Bayesian update of  
 370 the variances using the innovations. Building on Bocquet (2011); Bocquet et al. (2015); Ménétrier  
 371 and Auligné (2015), this technique was extended in Satterfield et al. (2018) to adaptively tune a  
 372 mixing ratio between the true and sample variances.

373 Adaptive covariance inflations are estimation methods directly attached to a traditional filtering  
 374 method (such as the EnKF used here), with almost negligible overhead computational cost. In  
 375 practice, the use of this technique does not necessarily imply an additive error term  $\eta$  in Eq. (1).  
 376 Thus, it is not a direct estimation of  $\mathbf{Q}$  but rather an inflation applied to  $\mathbf{P}^f$  in order to compensate  
 377 for model uncertainties and sampling errors in the EnKFs, as explained in Raanes et al. (2019,  
 378 their section 4 and appendix C). Several DA systems work with an inflation method and use it for  
 379 its simplicity, low cost, and efficiency. As an example of inflation techniques, the most straight-  
 380 forward inflation estimation is a multiplicative factor  $\lambda$  of the incorrectly scaled  $\tilde{\mathbf{P}}^f(k)$ , so that the  
 381 corrected forecast covariance is given by  $\mathbf{P}^f(k) = \lambda(k)\tilde{\mathbf{P}}^f(k)$ . The estimate of the inflation factor  
 382 is given by taking the trace of Eq. (6a):

$$\tilde{\lambda}(k) = \frac{\mathbf{d}^{o-f}(k)^T \mathbf{d}^{o-f}(k) - \text{Tr}(\mathbf{R}(k))}{\text{Tr}(\mathbf{H}_k \tilde{\mathbf{P}}^f(k) \mathbf{H}_k^T)}. \quad (8)$$

383 The estimated inflation parameter  $\tilde{\lambda}$  computed at each time  $k$  can be noisy. The use of temporal  
 384 smoothing of the form  $\lambda(k+1) = \rho \tilde{\lambda}(k) + (1 - \rho)\lambda(k)$  is crucial in operational procedures. Al-  
 385 ternatively, Miyoshi (2011) proposed calculating the estimated variance of  $\lambda(k)$ , denoted as  $\sigma_{\lambda(k)}^2$ ,  
 386 using the central limit theorem. Then,  $\lambda(k+1)$  is updated using the previous estimate  $\lambda(k)$  and  
 387 the Gaussian distribution with mean  $\tilde{\lambda}(k)$  and variance  $\sigma_{\lambda(k)}^2$ . From the Desroziers diagnostics,  
 388 at each time step  $k$  and when sufficient observations are available, an estimate of  $\mathbf{R}(k)$  is possible  
 389 using Eq. (6b). For instance, Li et al. (2009) proposed estimating each component of a diagonal

390 and averaged  $\mathbf{R}$  matrix. However, the diagonal terms cannot take into account spatial correlated  
391 error terms, and constant values for observation errors are not realistic. Then, Miyoshi et al. (2013)  
392 proposed additionally estimating the off-diagonal components of the time-dependent matrix  $\mathbf{R}(k)$ .  
393 The Miyoshi et al. (2013) implementation is summarized in the appendix, Algorithm 1.

394 The Desroziers diagnostic method has been applied widely to estimate the real observation error  
395 covariance matrix  $\mathbf{R}$  in Numerical Weather Prediction (NWP). The observations are coming from  
396 different sources. In the case of satellite radiances, Bormann et al. (2010) applied three meth-  
397 ods, including the Desroziers diagnostic and the method detailed in Hollingsworth and Lönnberg  
398 (1986) to estimate a constant diagonal term of  $\mathbf{R}$  using the innovation  $\mathbf{d}^{o-f}$  and its correlations  
399 in space, assuming that horizontal correlations in  $\mathbf{d}^{o-f}$  samples are purely due to  $\mathbf{P}^f$ . Weston  
400 et al. (2014) and Campbell et al. (2017) then included the inter-channel observation error correla-  
401 tions of satellite radiances in DA and obtained improved results compared with the case using a  
402 diagonal  $\mathbf{R}$ . For spatial error correlations in  $\mathbf{R}$ , Kotsuki et al. (2017a) estimated the horizontal ob-  
403 servation error correlations of satellite-derived precipitation data. Including horizontal observation  
404 error correlations in DA for densely-observed data from satellites and radars is more challenging  
405 than including inter-channel error correlations in DA. Indeed, the number of horizontally error-  
406 correlated observations is much larger, and some recent studies have been tackling this issue (e.g.,  
407 Guillet et al. (2019)).

408 To conclude, the Desroziers diagnostic is a consistency check and makes it possible to detect if  
409 the error covariances  $\mathbf{P}^f$  and  $\mathbf{R}$  are incorrect. When and how this method can result in accurate  
410 or inaccurate estimates, and convergence properties, have been studied in depth by Waller et al.  
411 (2016) and Ménard (2016). The Desroziers diagnostic is also useful to estimate off-diagonal terms  
412 of  $\mathbf{R}$ , for instance taking into account the spatial error correlations. However, covariance localiza-

413 tion used in the ensemble Kalman filter might induce erroneous estimates of spatial correlations  
414 (Waller et al. 2017).

415 *b. Lag innovation between consecutive times*

416 Another way to estimate error covariances is to use multiple equations involving  $\mathbf{Q}$  and  $\mathbf{R}$ ,  
417 exploiting cross-correlations between lag innovations. More precisely, it involves the current in-  
418 novation  $\mathbf{d}(k) = \mathbf{d}^{o-f}(k)$  defined in Eq. (4b) and past innovations  $\mathbf{d}(k-1), \dots, \mathbf{d}(k-l)$ . Lag  
419 innovations were introduced by Mehra (1970) to recover  $\mathbf{Q}$  and  $\mathbf{R}$  simultaneously for Gaussian,  
420 linear and stationary dynamic systems. In such a case,  $\{\mathbf{d}(k)\}_{k \geq 1}$  is completely characterized by  
421 the lagged covariance matrix  $\mathbf{C}_l = \text{Cov}(\mathbf{d}(k), \mathbf{d}(k-l))$ , which is independent of  $k$ . In other words,  
422 the information encoded in  $\{\mathbf{d}(k)\}_{k \geq 1}$  is completely equivalent to the information provided by  
423  $\{\mathbf{C}_l\}_{l \geq 0}$ . Moreover, for linear systems in a steady state, analytic relations exist between  $\mathbf{Q}$ ,  $\mathbf{R}$  and  
424  $E[\mathbf{d}(k)\mathbf{d}(k-l)^T]$ . However, these linear relations can be dependent and redundant for different  
425 lags  $l$ . Therefore, as stated in Mehra (1970), only a limited number of  $\mathbf{Q}$  components can be  
426 recovered.

427 Bélanger (1974) extended these results to the case of time-varying linear stochastic processes,  
428 taking  $\mathbf{d}(k)\mathbf{d}(k-l)^T$  as “observations” of  $\mathbf{Q}$  and  $\mathbf{R}$  and using a secondary Kalman filter to update  
429 them iteratively. On the one hand, considering the time-varying case may increase the number of  
430 components in  $\mathbf{Q}$  that can be estimated. On the other hand, as pointed out in Bélanger (1974),  
431 this method would no longer be analytically exact if  $\mathbf{Q}$  and  $\mathbf{R}$  were updated adaptively at each  
432 time step. One numerical difficulty of Bélanger’s method is that it needs to invert a matrix of size  
433  $m^2 \times m^2$ , where  $m$  refers to the dimension of the observation vector. However, this difficulty has  
434 been largely overcome by Dee et al. (1985) in which the matrix inversion is reduced to  $\mathcal{O}(m^3)$ , by  
435 taking the advantage of the fact that the big matrix comes from some tensor product.



436 More recent work have focused on high-dimensional and nonlinear systems using the extended  
 437 or ensemble Kalman filters. Berry and Sauer (2013) proposed a fast and adaptive algorithm in-  
 438 spired by the use of lag innovations proposed by Mehra. Harlim et al. (2014) applied the original  
 439 B elanger algorithm empirically to a nonlinear system with sparse observations. Zhen and Harlim  
 440 (2015) proposed a modified version of B elanger’s method, by removing the secondary filter and  
 441 alternatively solving  $\mathbf{Q}$  and  $\mathbf{R}$  in a least-squares sense based on the averaged linear relation over a  
 442 long term.

Here, we briefly describe the algorithm of Berry and Sauer (2013), considering the lag-zero and lag-one innovations. The following equations are satisfied in the linear and Gaussian case, for unbiased forecast and observation when  $\mathbf{P}^f(k)$  and  $\mathbf{R}(k)$  are correctly specified:

$$\begin{cases} \mathbf{E} [\mathbf{d}(k)\mathbf{d}(k)^T] = \mathbf{H}_k\mathbf{P}^f(k)\mathbf{H}_k^T + \mathbf{R}(k) = \mathbf{\Sigma}(k) & (9a) \\ \mathbf{E} [\mathbf{d}(k)\mathbf{d}(k-1)^T] = \mathbf{H}_k\mathbf{M}_k\mathbf{P}^f(k-1)\mathbf{H}_{k-1}^T & \\ -\mathbf{H}_k\mathbf{M}_k\mathbf{K}^f(k-1)\mathbf{\Sigma}(k-1). & (9b) \end{cases}$$

443 Equation (9a) is equivalent to Eq. (6a). Moreover, Eq. (9b) results from the fact that developing  
 444 the expression of  $\mathbf{d}(k)$  using consecutively Eqs. (2), (1), (4a), and (4d), the innovation can be  
 445 written as

$$\begin{aligned} \mathbf{d}(k) &= \mathbf{y}(k) - \mathbf{H}_k\mathbf{x}^f(k) \\ &= \mathbf{H}_k \left( \mathbf{x}(k) - \mathbf{x}^f(k) \right) + \boldsymbol{\epsilon}(k) \\ &= \mathbf{H}_k \left( \mathbf{M}_k\mathbf{x}(k-1) - \mathbf{x}^f(k) + \boldsymbol{\eta}(k) \right) + \boldsymbol{\epsilon}(k) \\ &= \mathbf{H}_k \left( \mathbf{M}_k \left( \mathbf{x}(k-1) - \mathbf{x}^a(k-1) \right) + \boldsymbol{\eta}(k) \right) + \boldsymbol{\epsilon}(k) \\ &= \mathbf{H}_k\mathbf{M}_k \left( \mathbf{x}(k-1) - \mathbf{x}^f(k-1) - \mathbf{K}^f(k-1)\mathbf{d}(k-1) \right) \\ &\quad + \mathbf{H}_k\boldsymbol{\eta}(k) + \boldsymbol{\epsilon}(k). \end{aligned} \tag{10}$$

446 Hence, the innovation product  $\mathbf{d}(k)\mathbf{d}(k-1)^T$  between two consecutive times is given by

$$\begin{aligned} & \mathbf{H}_k \mathbf{M}_k \left( \mathbf{x}(k-1) - \mathbf{x}^f(k-1) \right) \mathbf{d}(k-1)^T \\ & - \mathbf{H}_k \mathbf{M}_k \left( \mathbf{K}^f(k-1) \mathbf{d}(k-1) \right) \mathbf{d}(k-1)^T \\ & + \mathbf{H}_k \boldsymbol{\eta}(k) \mathbf{d}(k-1)^T + \boldsymbol{\epsilon}(k) \mathbf{d}(k-1)^T, \end{aligned} \quad (11)$$

447 and assuming that the model  $\boldsymbol{\eta}$  and observation  $\boldsymbol{\epsilon}$  error noises are white and mutually uncorrelated,  
 448 then  $E[\boldsymbol{\eta}(k)\mathbf{d}(k-1)^T] = 0$  and  $E[\boldsymbol{\epsilon}(k)\mathbf{d}(k-1)^T] = 0$ . Finally, developing  $E[\mathbf{d}(k)\mathbf{d}(k-1)^T]$ ,  
 449 Eq. (9b) is satisfied.

450 The algorithm in Berry and Sauer (2013) is summarized in the appendix, Algorithm 2. It is  
 451 based on an adaptive estimation of  $\mathbf{Q}(k)$  and  $\mathbf{R}(k)$ , which satisfies the following relations in the  
 452 linear and Gaussian case:

$$\begin{aligned} \tilde{\mathbf{P}}(k) &= (\mathbf{H}_k \mathbf{M}_k)^{-1} \mathbf{d}(k) \mathbf{d}(k-1)^T \mathbf{H}_{k-1}^{-T}, \\ &+ \mathbf{K}^f(k-1) \mathbf{d}(k-1) \mathbf{d}(k-1)^T \mathbf{H}_{k-1}^{-T} \end{aligned} \quad (12a)$$

$$\tilde{\mathbf{Q}}(k) = \tilde{\mathbf{P}}(k) - \mathbf{M}_{k-1} \mathbf{P}^a(k-2) \mathbf{M}_{k-1}^T, \quad (12b)$$

$$\tilde{\mathbf{R}}(k) = \mathbf{d}(k) \mathbf{d}(k)^T - \mathbf{H}_k \mathbf{P}^f(k) \mathbf{H}_k^T. \quad (12c)$$

453 In operational applications, when the number of observations is not equal to the number of  
 454 components in state  $\mathbf{x}$ ,  $\mathbf{H}$  is not a square matrix and Eq. (12a) is ill-defined. To avoid the inversion  
 455 of  $\mathbf{H}$ , Berry and Sauer (2013) proposed considering parametric models for  $\mathbf{Q}$  and then solving a  
 456 linear system associated with Eqs. (12a) and (12b). It is written as a least-squares problem such

457 that

$$\begin{aligned}
 \tilde{\mathbf{Q}}(k) = \arg \min_{\mathbf{Q}} & \|\mathbf{d}(k)\mathbf{d}(k-1)^T \\
 & + \mathbf{H}_k \mathbf{M}_k \mathbf{K}^f(k-1)\mathbf{d}(k-1)\mathbf{d}(k-1)^T \\
 & - \mathbf{H}_k \mathbf{M}_k \mathbf{M}_{k-1} \mathbf{P}^a(k-2) \mathbf{M}_{k-1}^T \mathbf{H}_{k-1}^T \\
 & - \mathbf{H}_k \mathbf{M}_k \mathbf{Q} \mathbf{H}_{k-1}^T \|.
 \end{aligned} \tag{13}$$

458 In this adaptive procedure, joint estimations of  $\tilde{\mathbf{Q}}(k)$  and  $\tilde{\mathbf{R}}(k)$  can abruptly vary over time.  
 459 Thus, the temporal smoothing of the covariances being estimated becomes crucial. As suggested  
 460 by Berry and Sauer (2013), such temporal smoothing between current and past estimates is a  
 461 reasonable choice:

$$\mathbf{Q}(k+1) = \rho \tilde{\mathbf{Q}}(k) + (1-\rho)\mathbf{Q}(k), \tag{14a}$$

$$\mathbf{R}(k+1) = \rho \tilde{\mathbf{R}}(k) + (1-\rho)\mathbf{R}(k) \tag{14b}$$

462 with  $\mathbf{Q}(1)$  and  $\mathbf{R}(1)$  the initial conditions and  $\rho$  the smoothing parameter. When  $\rho$  is large (close  
 463 to 1), weight is given to the current estimates  $\tilde{\mathbf{Q}}$  and  $\tilde{\mathbf{R}}$ , and when  $\rho$  is small (close to 0) it gives  
 464 smoother  $\mathbf{Q}$  and  $\mathbf{R}$  sequences. The value of  $\rho$  is arbitrary and may depend on the system and how  
 465 it is observed. For instance, in the case where the number of observations equals the size of the  
 466 system, Berry and Sauer (2013) uses  $\rho = 5 \times 10^{-5}$  in order to estimate the full matrix  $\mathbf{Q}$  for the  
 467 Lorenz-96 model.

468 The algorithm in Berry and Sauer (2013) only considers lag-zero and lag-one innovations. By  
 469 incorporating more lags, Zhen and Harlim (2015) and Harlim (2018) showed that it makes it  
 470 possible to deal with the case in which some components of  $\mathbf{Q}$  are not identifiable from the method  
 471 in Berry and Sauer (2013). For instance, let us consider the two-dimensional system with any  
 472 stationary operator  $\mathbf{M}$  and  $\mathbf{H} = [1, 0]$ , meaning that only the first component of the system is

473 observed. This is a linear, Gaussian, stationary system, and Mehra's theory implies that two  
474 parameters of  $\mathbf{Q}$  are identifiable. However, using only lag-one innovations as in Berry and Sauer  
475 (2013), Eq. (13) becomes a scalar equation and only one parameter of  $\mathbf{Q}$  can be determined. The  
476 idea of considering more lag innovations to estimate more components of  $\mathbf{Q}$  was tested in Zhen  
477 and Harlim (2015). Numerical results show that considering more than one lag can improve the  
478 estimates of  $\mathbf{Q}$  and  $\mathbf{R}$ . For instance, Zhen and Harlim (2015) focused on the Lorenz-96 model.  
479 Results show that when  $\mathbf{Q}$  is stationary, the trace of  $\mathbf{Q}$  and  $\mathbf{R}$  are equal, and when observations are  
480 taken at twenty fixed equally spaced grid points for every five integration time steps, the optimal  
481 RMSE of the estimates of  $\mathbf{Q}$  and  $\mathbf{R}$  is achieved when four time lags are considered. But with more  
482 lags, the performance is degraded.

483 To summarize, methods based on lag innovation between consecutive times have been studied  
484 for a long time in the signal processing community. The original methods (Mehra 1970; Bélanger  
485 1974) were analytically established for linear systems with Gaussian noises. Inspired by these  
486 foundational ideas, empirical methods have been established for nonlinear systems in DA (Berry  
487 and Sauer 2013; Harlim et al. 2014; Zhen and Harlim 2015). Although these methods have not  
488 been tested in any operational experiment, the idea of using lagged innovations seems to have  
489 significant potential.

#### 490 **4. Likelihood-based methods**

491 This section focuses on methods based on the likelihood of the observations, given a set of  
492 statistical parameters. The conceptual idea behind what we refer to as likelihood-based methods  
493 is to determine the optimal statistical parameters (i.e.,  $\mathbf{Q}$  and  $\mathbf{R}$ ) that maximize the likelihood  
494 function for a given set of observations which may be distributed over time. In this way, the aim

495 is to derive estimation methods that use the observations to find the most suitable, or most likely  
496 parameters.

497 Early studies in Dee (1995), Blanchet et al. (1997), Mitchell and Houtekamer (2000) and Liang  
498 et al. (2012) proposed finding the optimal  $\mathbf{Q}$  and  $\mathbf{R}$  that maximize the current innovation likelihood  
499 at time  $k$ . Unfortunately, if only the current observations are used, the joint estimation of  $\mathbf{Q}$  and  $\mathbf{R}$   
500 is not well constrained (Todling 2015). To tackle this issue, several solutions have been recently  
501 proposed where the likelihood function considers observations distributed in time over several  
502 assimilation cycles.

503 The likelihood-based methods are broadly divided into two categories. One approach uses a  
504 Bayesian framework. It assumes a priori knowledge about the parameters and estimate jointly the  
505 posterior distribution of  $\mathbf{Q}$  and  $\mathbf{R}$  together with the state of the system, or alternatively to estimate  
506 them in a two-stage process<sup>2</sup>. The second one is based on the frequentist viewpoint and attempts  
507 a point estimate of the parameters by maximizing a total likelihood function.

#### 508 *a. Bayesian inference*

509 In the Bayesian framework, the elements of the covariance matrices  $\mathbf{Q}$  and  $\mathbf{R}$  are assumed to  
510 have a priori distributions which are controlled by hyperparameters. In practice, it is difficult to  
511 have prior distributions for each element of  $\mathbf{Q}$  and  $\mathbf{R}$ , especially for large DA systems. Instead,  
512 parametric forms are used for the matrices, typically describing the shape and level noise. We  
513 denote the corresponding parameters as  $\theta$ .

---

<sup>2</sup>Some of the methods presented in section 3 also use the Bayesian philosophy; for instance they assume a priori distribution for the multiplicative inflation parameter  $\lambda$  (Anderson 2009; El Gharamti 2018).

514 The inference in the Bayesian framework aims to determine the posterior density  $p(\boldsymbol{\theta}|\mathbf{y}(1:k))$ .  
515 Two techniques have appeared, the first based on a state augmentation and the second based on a  
516 rigorous Bayesian update of the posterior distribution.

## 517 1) STATE AUGMENTATION

518 In the Bayesian framework,  $\boldsymbol{\theta}$  is a random variable such that the state is augmented with these  
519 parameters by defining  $\mathbf{z}(k) = (\mathbf{x}(k), \boldsymbol{\theta})$ . To define an augmented state-space model, one has to  
520 define an evolution equation for the parameters. This leads to a new state-space model of the form  
521 of Eqs. (1) and (2) with  $\mathbf{x}$  replaced by  $\mathbf{z}$ . Therefore, the state and the parameters are estimated  
522 jointly using the DA algorithms.

523 State augmentation was first proposed in Schmidt (1966) and is known as the Schmidt–Kalman  
524 filter. This technique was mainly used to estimate both the state of the system and additional pa-  
525 rameters, including bias, forcing terms and physical parameters. These kinds of parameters are  
526 strongly related to the state of the system (Ruiz et al. 2013a). Therefore, they are identifiable  
527 and suitable for an augmented state approach. However, Stroud and Bengtsson (2007) and later  
528 Delsole and Yang (2010) formally demonstrated that augmentation methods fail for variance pa-  
529 rameters like  $\mathbf{Q}$  and  $\mathbf{R}$ . The explanation is that in the EnKF, the empirical forecast covariance  $\mathbf{P}^f$   
530 is computed using all the ensemble members, each one with a different realization of the random  
531 variable  $\boldsymbol{\theta}$ . Thus,  $\mathbf{P}^f$  and consequently the Kalman gain  $\mathbf{K}^f$ , are mixing the effects of  $\mathbf{Q}$  and  $\mathbf{R}$   
532 parameters contained in  $\boldsymbol{\theta}$ . Therefore, after applying Eq. (4d), the update of  $\mathbf{z}$  corresponding to  
533 the  $\boldsymbol{\theta}$  parameters is the same for all the parameters. To capture the impact of a single variance  
534 parameter on the prediction covariance and circumvent the limitation of the state augmentation,  
535 Scheffler et al. (2019) proposed to use an ensemble of states integrated with the same variance  
536 parameter. The choice of an ensemble of states for each variance parameter leads to two nested

537 ensemble Kalman filters. The technique performs successfully under different model error covari-  
538 ance structures but has an important computational cost.

539 Another critical aspect of state augmentation is that one needs to define an evolution model for  
540 the augmented state  $\mathbf{z}(k) = (\mathbf{x}(k), \boldsymbol{\theta}(k))$ . If persistence is assumed in the parameters such that they  
541 are constant in time, this leads to filter degeneracy, since the estimated variance of the error in  $\boldsymbol{\theta}$   
542 is bound to decrease in time. To prevent or at least mitigate this issue, it was suggested to use an  
543 independent inflation factor on the parameters (Ruiz et al. 2013b) or to impose artificial stochastic  
544 dynamics for  $\boldsymbol{\theta}$ , typically a random walk or AR(1) model, as introduced in Eq. (3) and proposed  
545 in Liu and West (2001). The tuning of the parameters introduced in these artificial dynamics may  
546 be difficult, and this introduces bias into the procedure, which is hard to quantify.

## 547 2) BAYESIAN UPDATE OF THE POSTERIOR DISTRIBUTION

548 Instead of the inference of the joint posterior density using a state augmentation strategy, the  
549 state  $\mathbf{x}(k)$  and parameters  $\boldsymbol{\theta}$  can be divided into a two-step inference procedure using the following  
550 formula:

$$\begin{aligned} p(\mathbf{x}(k), \boldsymbol{\theta} | \mathbf{y}(1:k)) = \\ p(\mathbf{x}(k) | \mathbf{y}(1:k), \boldsymbol{\theta}) p(\boldsymbol{\theta} | \mathbf{y}(1:k)), \end{aligned} \quad (15)$$

551 which is a direct consequence of the conditional density definition. In Eq. (15),  $p(\mathbf{x}(k) | \mathbf{y}(1:k), \boldsymbol{\theta})$   
552 represents the posterior distribution of the state, given the observations and the parameter  $\boldsymbol{\theta}$ . It can  
553 be computed using a filtering DA algorithm. The second term on the right-hand side of Eq. (15)  
554 corresponds to the posterior distribution of the parameters, given the observations up to time  $k$ .

555 The latter can be updated sequentially using the following Bayesian hierarchy:

$$p(\boldsymbol{\theta}|\mathbf{y}(1:k)) \propto p(\mathbf{y}(k)|\mathbf{y}(1:k-1), \boldsymbol{\theta}) p(\boldsymbol{\theta}|\mathbf{y}(1:k-1)), \quad (16)$$

556 where  $p(\mathbf{y}(k)|\mathbf{y}(1:k-1), \boldsymbol{\theta})$  is the likelihood of the innovations.

557 Different approximations have been used for  $p(\boldsymbol{\theta}|\mathbf{y}(1:k))$  in Eq. (16); these include parametric  
558 models based on Gaussian (Stroud et al. 2018), inverse-gamma (Stroud and Bengtsson 2007) or  
559 Wishart distributions (Ueno and Nakamura 2016), particle-based approximations (Frei and Künsch  
560 2012; Stroud et al. 2018) and grid-based approximation (Stroud et al. 2018).

561 The methods proposed in the literature also differ by the approximation used for the likelihood  
562 of the innovations. We emphasize that  $p(\mathbf{y}(k)|\mathbf{y}(1:k-1), \boldsymbol{\theta})$  needs to be evaluated for different  
563 values of  $\boldsymbol{\theta}$  at each time step, and that this requires applying the filter from the initial time with  
564 a single value of  $\boldsymbol{\theta}$ , which is computationally impossible for applications in high dimensions. To  
565 reduce computational time, it is generally assumed that  $\mathbf{x}^f$  and  $\mathbf{P}^f$  are independent of  $\boldsymbol{\theta}$ , and only  
566 observations  $\mathbf{y}(k-l:k-1)$  in a small time window from the current observation are used when  
567 computing the likelihood of the innovations (see Ueno and Nakamura (2016); Stroud et al. (2018)  
568 for a more detailed discussion). A summary of the Bayesian method from Stroud et al. (2018) is  
569 given in the appendix, Algorithm 3. It was implemented within the EnKF framework and is one  
570 of the most recent studies based on the Bayesian approach.

571 Applications of the Bayesian methodology in the DA context are now discussed. It has mainly  
572 been used to estimate shape and noise parameters of  $\mathbf{Q}$  and  $\mathbf{R}$  error covariance matrices. For  
573 instance, Purser and Parrish (2003) and Solonen et al. (2014) estimated statistical parameters con-  
574 trolling the magnitude of the variance and the spatial dependencies in the model error  $\mathbf{Q}$ , assuming  
575 that  $\mathbf{R}$  is known. There are also applications aimed at estimating parameters governing the shape



576 of the observation error covariance matrix  $\mathbf{R}$  only: Frei and Künsch (2012) and Stroud et al. (2018)  
577 in the Lorenz-96 system, Winiarek et al. (2012, 2014) for the inversion of the source term of air-  
578 borne radionuclides using a regional atmospheric model, and Ueno and Nakamura (2016) using a  
579 shallow-water model to assimilate satellite altimetry.

580 As pointed out in Stroud and Bengtsson (2007), Bayesian update algorithms work best when the  
581 number of unknown parameters in  $\theta$  is small. This limitation may explain why the joint estimation  
582 of parameters controlling both model and observation error covariances is not systematically ad-  
583 dressed. For instance, Stroud and Bengtsson (2007) used the EnKF with the Lorenz-96 model for  
584 the estimation of a common multiplicative scalar parameter for predefined matrices  $\mathbf{Q}$  and  $\mathbf{R}$ . Al-  
585 ternatively, Stroud et al. (2018) tested the Bayesian method on different spatio-temporal systems  
586 to estimate the signal-to-noise ratio between  $\mathbf{Q}$  and  $\mathbf{R}$ . Nevertheless, based on the experiments  
587 about the importance of the signal-to-noise ratio  $\|\mathbf{P}^f\| / \|\mathbf{R}\|$  presented in Fig. 2, we know that this  
588 estimation of the ratio is not optimal.

589 Widely used in the statistical community, the Bayesian framework is useful incorporating phys-  
590 ical knowledge about error covariance matrices and constraining their estimation process. In the  
591 DA literature, authors have used a priori distributions for the shape and noise parameters of  $\mathbf{Q}$   
592 or  $\mathbf{R}$ , but rarely both. Operationally, only a limited number of parameters can be estimated. To  
593 address this issue, Stroud and Bengtsson (2007) suggested combining Bayesian algorithms with  
594 other techniques.

### 595 *b. Maximization of the total likelihood.*

596 The innovation likelihood at time  $k$ ,  $p(\mathbf{y}(k)|\mathbf{y}(1:k-1), \theta)$  in Eq. (16), can be maximized to  
597 find the optimal  $\theta$  (i.e.,  $\mathbf{Q}$  and  $\mathbf{R}$  matrices or parameterizations of them). In practice, when this  
598 maximization is done at each time step, two issues arise. Firstly, the innovation covariance matrix

599  $\Sigma(k) = \mathbf{H}_k \mathbf{P}^f(k) \mathbf{H}_k^T + \mathbf{R}(k)$  combines the information about  $\mathbf{R}$  and  $\mathbf{Q}$ , the latter being contained  
600 in  $\mathbf{P}^f$ . When using only time  $k$ , it is difficult to disentangle the model and observation error  
601 covariances; in application, the aforementioned studies only estimated one of them. Secondly,  
602 the number of observations at each time step is in general limited and, as pointed out by Dee  
603 (1995), available observations should exceed “the number of tunable parameters by two or three  
604 orders of magnitude”. To overcome these limitations, a reasonable alternative is to use a batch of  
605 observations within a time window and to assume  $\theta$  to be constant in time. The resulting total  
606 likelihood expressed sequentially through conditioning is given by

$$p(\mathbf{y}(1:K)|\theta) = \prod_{k=1}^K p(\mathbf{y}(k)|\mathbf{y}(1:k-1), \theta). \quad (17)$$

607 Because it is an integration of innovation likelihoods over a long period of time from  $k = 1$  to  $k =$   
608  $K$ , Eq. (17) provides more observational information to estimate  $\mathbf{Q}$  and  $\mathbf{R}$ . The maximization of  
609 this total likelihood has been applied for the estimation of deterministic and stochastic parameters  
610 (related to  $\mathbf{Q}$ ) using a direct sequential optimization procedure (Delsole and Yang 2010). Ueno  
611 et al. (2010) used a grid-based procedure to estimate noise levels and spatial correlation lengths of  
612  $\mathbf{Q}$  and a noise level for  $\mathbf{R}$ . This grid-based method uses predefined sets of covariance parameters  
613 and evaluates the different combinations to find the one that maximizes the likelihood criterion.  
614 Brankart et al. (2010) also proposed a method using the same criterion but adding (at the initial  
615 time) information on scale and correlation length parameters of  $\mathbf{Q}$  and  $\mathbf{R}$ . This information is only  
616 given the first time, and is progressively forgotten over time, using a decreasing exponential factor.  
617 The marginalization of the hidden state in Eq. (17) considers all the previous observations, and it  
618 requires the use of a filter. The maximization of the total likelihood  $p(\mathbf{y}(1:K)|\theta)$  to estimate  
619 model error covariance  $\mathbf{Q}$  was conducted in Pulido et al. (2018), where they used a gradient-based  
620 optimization technique and the EnKF.

621 The likelihood function given in Eq. (17) only depends on the observations  $\mathbf{y}$ . This likelihood  
 622 can be written in a different way, taking into account both the observations and the hidden state  $\mathbf{x}$ .  
 623 Indeed, the marginalization of the hidden state to obtain the total likelihood can be produced using  
 624 the whole trajectory of the state from  $k = 0$  to the last time step  $K$  all at once. It is given by

$$p(\mathbf{y}(1:K)|\boldsymbol{\theta}) = \int p(\mathbf{x}(0:K), \mathbf{y}(1:K)|\boldsymbol{\theta}) d\mathbf{x}(0:K). \quad (18)$$

625 The maximization of the total likelihood as a function of statistical parameters  $\boldsymbol{\theta}$  is not possible,  
 626 since the total likelihood cannot be evaluated directly, nor its gradient with regard to the parameters  
 627 (Pulido et al. 2018). Shumway and Stoffer (1982) proposed using an iterative procedure based on  
 628 the expectation–maximization algorithm (hereinafter denoted as EM). They applied it to estimate  
 629 the parameters of a linear state-space model, with linear dynamics, and a linear observational  
 630 operator and Gaussian errors. The EM algorithm was introduced by Dempster et al. (1977).

631 Each iteration of the EM algorithm consists of two steps. In the expectation step (E-step), the  
 632 posterior density  $p(\mathbf{x}(0:K)|\mathbf{y}(1:K), \boldsymbol{\theta}_{(n)})$  is determined conditioned on the batch of observations  
 633  $\mathbf{y}(1:K)$  and given the parameters  $\boldsymbol{\theta}_{(n)} = (\mathbf{Q}_{(n)}, \mathbf{R}_{(n)})$  from the previous iteration or initial guess.  
 634 This is obtained through the application of a smoother like the EnKS. Then, the M-step relies on  
 635 the maximization of an intermediate function, depending on the posterior density obtained in the  
 636 E-step. The intermediate function is defined by the conditional expectation

$$\mathbb{E} [\log(p(\mathbf{x}(0:K), \mathbf{y}(1:K)|\boldsymbol{\theta})) | \mathbf{y}(1:K), \boldsymbol{\theta}_{(n)})]. \quad (19)$$

637 If as in Eqs. (1) and (2) the observational and model errors are assumed to be additive, unbiased  
 638 and Gaussian, the expression for the logarithm of the joint density in Eq. (19) is given by

$$\begin{aligned} & -\frac{1}{2} \left\{ \sum_{k=1}^K \|\mathbf{x}(k) - \mathcal{M}(\mathbf{x}(k-1))\|_{\mathbf{Q}}^2 + \log |\mathbf{Q}| \right. \\ & \left. + \|\mathbf{y}(k) - \mathcal{H}(\mathbf{x}(k))\|_{\mathbf{R}}^2 + \log |\mathbf{R}| \right\} + c \end{aligned} \quad (20)$$

639 where  $\|\mathbf{v}\|_{\mathbf{A}}^2$  is defined to be equal to  $\mathbf{v}^T \mathbf{A}^{-1} \mathbf{v}$  and  $c$  is a constant independent of  $\mathbf{Q}$  and  $\mathbf{R}$ . In this  
 640 case, an analytic expression for the optimal error covariances at each iteration of the EM algorithm  
 641 can be obtained. The estimators of the parameters that maximize Eq. (19) using Eq. (20) are

$$\mathbf{Q}_{(n+1)} = \frac{1}{K} \sum_{k=1}^K \mathbb{E}[(\mathbf{x}(k) - \mathcal{M}(\mathbf{x}(k-1))) (\mathbf{x}(k) - \mathcal{M}(\mathbf{x}(k-1)))^T | \mathbf{y}(1:K), \boldsymbol{\theta}_{(n)}] \quad (21a)$$

642 and

$$\mathbf{R}_{(n+1)} = \frac{1}{K} \sum_{k=1}^K \mathbb{E}[(\mathbf{y}(k) - \mathcal{H}(\mathbf{x}(k))) (\mathbf{y}(k) - \mathcal{H}(\mathbf{x}(k)))^T | \mathbf{y}(1:K), \boldsymbol{\theta}_{(n)}]. \quad (21b)$$

643 The application of the EM algorithm for the estimation of  $\mathbf{Q}$  and  $\mathbf{R}$  is rather straightforward.  
 644 Starting from  $\mathbf{Q}_{(1)}$  and  $\mathbf{R}_{(1)}$ , an ensemble Kalman smoother is applied with this first guess and  
 645 the batch of observations  $\mathbf{y}(1:K)$  to obtain the posterior density  $p(\mathbf{x}(0:K) | \mathbf{y}(1:K), \boldsymbol{\theta}_{(1)})$ . Then  
 646 Eqs. (21a) and (21b) are used to update and obtain  $\mathbf{Q}_{(2)}$  and  $\mathbf{R}_{(2)}$ . Next, a new application of  
 647 the smoother is conducted using the parameters  $\mathbf{Q}_{(2)}$  and  $\mathbf{R}_{(2)}$  and the observations  $\mathbf{y}(1:K)$ , the  
 648 new resulting states are used in Eqs. (21a) and (21b) to estimate  $\mathbf{Q}_{(3)}$  and  $\mathbf{R}_{(3)}$ , and so on. As  
 649 a diagnostic of convergence or as a stop criterion, the product of innovation likelihood functions  
 650 given in Eq. (17) is evaluated using a filter. The EM algorithm guarantees that the total likelihood  
 651 increases in each iteration and that the sequence  $\boldsymbol{\theta}_{(n)}$  converges to a local maximum (Wu 1983).  
 652 A summary of the EM method (using EnKF and EnKS) from Dreano et al. (2017) is given in the  
 653 appendix, Algorithm 4.

654 EM is a well-known algorithm used in the statistical community. This procedure is parameter-  
 655 free and robust, due to the large number of observations used to approximate the likelihood when  
 656 using a long batch period (Shumway and Stoffer 1982). Although the use of the EM algorithm is

657 still limited in DA, it is becoming more and more popular. Some studies have implemented the EM  
658 algorithm for estimating only the observation error matrix  $\mathbf{R}$ . For instance, Ueno and Nakamura  
659 (2014) used the model proposed in Zebiak and Cane (1987) and satellite altimetry observations,  
660 whereas Liu et al. (2017) used an air quality model for accidental pollutant source retrieval. But  
661 the estimation of only the observation error covariance is limited, and other studies have tried  
662 to jointly estimate model error  $\mathbf{Q}$  and  $\mathbf{R}$  matrices, for instance as in Tandeo et al. (2015) for an  
663 orographic subgrid-scale nonlinear observation operator. Then, Dreano et al. (2017) and Pulido  
664 et al. (2018) used the EM procedure to produce joint estimation of  $\mathbf{Q}$  and  $\mathbf{R}$  matrices in the Lorenz-  
665 63 and stochastic parameters of the Lorenz-96 systems, respectively. Recently, Yang and Mémin  
666 (2019) extended the EM procedure for the estimation of physical parameters in a one-dimensional  
667 shallow water model, more specifically for the identification of stochastic subgrid terms. Lastly,  
668 an online adaptation of the EM algorithm for the estimation of  $\mathbf{Q}$  and  $\mathbf{R}$  at each time step, after the  
669 filtering procedure, has been proposed in Cocucci et al. (2020). In this adaptive case, the likelihood  
670 is averaged locally over time, see Cappé (2011) for more details.

671 To our knowledge, EM has not been tested yet on operational systems with large observation-  
672 and state-space. In that case, the use of parametric forms for the matrices  $\mathbf{Q}$  and  $\mathbf{R}$  is essential to  
673 reduce the number of statistical parameters  $\theta$  to estimate. For instance, Dreano et al. (2017) and  
674 Liu et al. (2017) showed that in the particular cases where covariances are diagonal or of the form  
675  $\alpha\mathbf{A}$  with  $\mathbf{A}$  a positive definite matrix, expressions in Eq. (21a) and Eq. (21b) are simplified, and a  
676 suboptimal  $\theta$  in the space of the parametric covariance form can be obtained.

## 677 **5. Other methods**

678 In this section, we describe other methods that have been used to estimate  $\mathbf{Q}$  and  $\mathbf{R}$ , and that  
679 cannot be included in the categories presented in the previous sections. In particular, we report

680 here about methods that are applied either a posteriori, after DA cycles, or without applying any  
681 DA algorithms.

682 *a. Analysis (or reanalysis) increment approach*

683 This first method is based on previous DA outputs. The key idea here is to use the analysis  
684 (or reanalysis) increments to provide a realistic sample of model errors from which statistical  
685 moments, such as the covariance matrix  $\mathbf{Q}$ , can be empirically estimated. This assumes that the  
686 sequence of reanalysis  $\mathbf{x}^s$  (or analysis  $\mathbf{x}^a$ ) is the best available representation of the true process  $\mathbf{x}$ .  
687 In that case, the following approximation in Eq. (1) is made:

$$\begin{aligned}\boldsymbol{\eta}(k) &= \mathcal{M}(\mathbf{x}(k-1)) - \mathbf{x}(k) \\ &\approx \mathcal{M}(\mathbf{x}^s(k-1)) - \mathbf{x}^s(k).\end{aligned}\tag{22}$$

688 In this approximation, it is implicitly assumed that the estimated state is the truth, so that the initial  
689 condition at time  $k-1$  is neglected. A similar approximation of the true process by  $\mathbf{x}^a$  or  $\mathbf{x}^s$  in  
690 Eq. (2) can be used to estimate the observation error covariance matrix  $\mathbf{R}$ .

691 Operationally, the analysis (or reanalysis) increment method is applied after a DA filter (or  
692 smoother) to estimate the  $\mathbf{Q}$  matrix. This method was originally introduced by Leith (1978), and  
693 later used to account for model error in the context of ensemble Kalman filters, using analysis and  
694 reanalysis increments by Mitchell and Carrassi (2015), and in the context of weak-constraint vari-  
695 ational assimilation by Bowler (2017). Along this line, Rodwell and Palmer (2007) also proposed  
696 evaluating the average of instantaneous analysis increments to represent the systematic forecast  
697 tendencies of a model.

698 *b. Covariance matching*

699 The covariance matching method was introduced by Fu et al. (1993). It involves matching  
 700 sample covariance matrices to their theoretical expectations. Thus, it is a method of moments,  
 701 similar to the work in Desroziers et al. (2005), except that covariance matching is performed  
 702 on a set of historical observations and numerical simulations (noted  $\mathbf{x}^{sim}$ ), without applying any  
 703 DA algorithms. It has been extended by Menemenlis and Chechelnitsky (2000) to time-lagged  
 704 innovations, as first considered in Bélanger (1974).

In the case of a constant and linear observation operator  $\mathbf{H}$ , the basic idea in Fu et al. (1993) is to assume the following system

$$\begin{cases} \mathbf{x}^{sim}(k) = \mathbf{x}(k) + \boldsymbol{\eta}^{sim}(k), & (23a) \\ \boldsymbol{\eta}^{sim}(k) = \mathbf{A}\boldsymbol{\eta}^{sim}(k-1) + \boldsymbol{\eta}(k), & (23b) \\ \mathbf{H}\mathbf{x}^{sim}(k) - \mathbf{y}(k) = \mathbf{H}\boldsymbol{\eta}^{sim}(k) + \boldsymbol{\epsilon}(k), & (23c) \end{cases}$$

705 with  $\mathbf{A}$  a transition matrix close to the identity matrix, assuming slow variations of the numerical  
 706 simulation errors (noted  $\boldsymbol{\eta}^{sim}$ ). In Eq. (23b) and Eq. (23c), the definitions of  $\boldsymbol{\eta}$  and  $\boldsymbol{\epsilon}$  errors remain  
 707 similar, as in the general Eqs. (1) and (2).

708 Assuming that  $\mathbf{Q}$  and  $\mathbf{R}$  are constant over time,  $\boldsymbol{\epsilon}$  is uncorrelated from  $\mathbf{x}$  and from  $\boldsymbol{\eta}^{sim}$ , then  
 709 Eq. (23c) and Eq. (23a) yield to the following estimates of  $\mathbf{R}$  and  $\mathbf{P}^{sim}$  (the latter represents the  
 710 error covariance of the numerical simulations):

$$\hat{\mathbf{R}} = \frac{1}{2} \{ \mathbb{E}[(\mathbf{y} - \mathbf{H}\mathbf{x}^{sim})(\mathbf{y} - \mathbf{H}\mathbf{x}^{sim})^T] - \mathbb{E}[(\mathbf{H}\mathbf{x}^{sim})(\mathbf{H}\mathbf{x}^{sim})^T] + \mathbb{E}[\mathbf{y}\mathbf{y}^T] \}, \quad (24a)$$

$$\mathbf{H}\hat{\mathbf{P}}^{sim}\mathbf{H}^T = \frac{1}{2} \{ \mathbb{E}[(\mathbf{y} - \mathbf{H}\mathbf{x}^{sim})(\mathbf{y} - \mathbf{H}\mathbf{x}^{sim})^T] + \mathbb{E}[(\mathbf{H}\mathbf{x}^{sim})(\mathbf{H}\mathbf{x}^{sim})^T] - \mathbb{E}[\mathbf{y}\mathbf{y}^T] \}. \quad (24b)$$

711 where  $E$  is the expectation operator over time. Then, an estimate of  $\mathbf{Q}$  is obtained using Eq. (23b),  
712 Eq. (24b) and assuming that  $\mathbf{P}^{sim}$  has a unique time-invariant limit.

### 713 *c. Forecast sensitivity*

714 In operational meteorology, it is critical to learn the sensitivity of the forecast accuracy to various  
715 parameters of a DA system, in particular the error statistics of both the model and the observations.  
716 This is why a significant portion of literature considers the tuning problem of  $\mathbf{R}$  and  $\mathbf{Q}$  through the  
717 lens of the sensitivity of the forecast to these parameters. The computation of those sensitivities can  
718 be seen as a first-order correction or diagnostic for such an estimation. The forecast sensitivities are  
719 computed either using the adjoint model (Daescu and Todling 2010; Daescu and Langland 2013)  
720 in the context of variational methods, or a forecast ensemble (Hotta et al. 2017) in the context of  
721 the EnKF.

722 The basic idea is to compute at each assimilation cycle an innovation between forecast and anal-  
723 ysis, noted  $\mathbf{d}^{f-a}(k) = \mathbf{x}^f(k) - \mathbf{x}^a(k)$ . Then, the forecast sensitivity is given by  $\mathbf{d}^{f-a}(k)^T \mathbf{S} \mathbf{d}^{f-a}(k)$   
724 with  $\mathbf{S}$  a diagonal scaling matrix, to normalize the components of  $\mathbf{d}^{f-a}$ .  $\mathbf{Q}$  and  $\mathbf{R}$  estimates are the  
725 matrices that minimize  $\mathbf{d}^{f-a}(k)$ . The adjoint or the ensemble are thus used to compute the partial  
726 derivatives of this forecast sensitivity. w.r.t.  $\mathbf{Q}$  and  $\mathbf{R}$ .

## 727 **6. Conclusions and perspectives**

728 As often considered in data assimilation, this review paper also deals with model and observation  
729 errors that are assumed additive and Gaussian with covariance matrices  $\mathbf{Q}$  and  $\mathbf{R}$ . The model error  
730 corresponds to the dynamic model deficiencies to represent the underlying physics, whereas the  
731 observation error corresponds to the instrumental noise and the representativity error. Model and



732 observation errors are assumed to be uncorrelated and white in time. The model and observations  
733 are also assumed unbiased, a strong assumption for real data assimilation applications.

734 The discussion starts with the aid of an illustration of the individual and joint impacts of im-  
735 properly calibrated covariances using a linear toy model. The experiments clearly showed that  
736 to achieve reasonable filter accuracy (i.e., in terms of root mean squared error), it is crucial to  
737 carefully define both  $\mathbf{Q}$  and  $\mathbf{R}$ . The effect on the coverage probability of a mis-specification of  
738  $\mathbf{Q}$  or  $\mathbf{R}$  is also highlighted. This coverage probability is related to the estimated covariance of  
739 the reconstructed state, and thus to the uncertainty quantification in data assimilation. After the  
740 one-dimensional illustration, the core of the paper gives an overview of various methods to jointly  
741 estimate the  $\mathbf{Q}$  and  $\mathbf{R}$  error covariance matrices: they are summarized and compared below.

#### 742 *a. Comparison of existing methods for estimating $\mathbf{Q}$ and $\mathbf{R}$*

743 We mainly focused in this review on four methodologies for the joint estimation of the error co-  
744 variances  $\mathbf{Q}$  and  $\mathbf{R}$ . The methods are summarized in Table 1. They correspond to classic estimation  
745 methods, based on statistical moments or likelihoods. The main difference between the four meth-  
746 ods comes from the innovations taken into account: the total innovation, as in the EM algorithm  
747 proposed by Shumway and Stoffer (1982); lag innovations, following the idea given in Mehra  
748 (1970); or different type of innovations in the observation space, as in Desroziers et al. (2005).  
749 Additionally, to constrain the estimation, hierarchical Bayesian approaches use prior distributions  
750 for the shape parameters of  $\mathbf{Q}$  and  $\mathbf{R}$ .

751 Most of the methods estimate the model error  $\mathbf{Q}$ . The exception is the one using the Desroziers  
752 diagnostic, dealing with different type of innovations in the observation space, which instead esti-  
753 mates an inflation factor for  $\mathbf{P}^f$ . Moreover, the methods are mainly defined online, meaning that  
754 they aim to estimate  $\mathbf{Q}$  and  $\mathbf{R}$  adaptively, together with the current state of the system. Conse-

755 quently, these methods require additional tunable parameters to smooth the estimated covariances  
756 over time. However, most of the methods presented in this review also have an offline variant. In  
757 that case, a batch of observations is used to estimate  $\mathbf{Q}$  and  $\mathbf{R}$ . In some methods, such as the EM  
758 algorithm, the parameters are determined iteratively. These offline approaches avoid the use of  
759 additional smoothing parameters.

760 Throughout this review paper, as usually stated in DA, it is assumed that model error  $\boldsymbol{\eta}$  and  
761 observation error  $\boldsymbol{\epsilon}$ , defined in Eqs. (1) and (2), are Gaussian. Consequently, the distribution of the  
762 innovations are also Gaussian. The four presented methods use this property to build estimates of  
763  $\mathbf{Q}$  and  $\mathbf{R}$  adequately. But, if  $\boldsymbol{\eta}$  and  $\boldsymbol{\epsilon}$  are non-Gaussian, Desroziers diagnostic and lag-innovation  
764 methods are not suitable anymore. However, the EM procedures and Bayesian methods are still  
765 relevant, although they must be used with an appropriate filter (e.g., particle filters), not Kalman-  
766 based algorithms (i.e., assuming a Gaussian distribution of the state). Recently, the treatment of  
767 non-Gaussian error distributions in DA has been explored in Katzfuss et al. (2019), using hierarchi-  
768 cal state-space models. This Bayesian framework allows to handle unknown variables that cannot  
769 be easily included in the state vector (e.g., parameters of  $\mathbf{Q}$  and  $\mathbf{R}$ ) and to model non-Gaussian  
770 observations.

771 The four methods have been applied at different levels of complexity. For instance, Bayesian  
772 inference methods (due to their algorithm complexity) and the EM algorithm (due to its computa-  
773 tional cost) have so far only been applied to small dynamic models. However, the online version of  
774 the EM algorithm is less consuming and opens new perspectives of applications on larger models.  
775 On the other hand, methods using innovation statistics in the observation space have already been  
776 applied to NWP models.

777 The four methods summarized in Table 1 show differences in maturity in terms of applications  
778 and methodological aspects. This review also shows that there are still remaining challenges and  
779 possible improvements for the four methods.

780 *b. Remaining challenges for each method*

781 The first challenge concerns the improvements of adaptive techniques regarding additional pa-  
782 rameters that control the variations of  $\mathbf{Q}$  and  $\mathbf{R}$  estimates over time. Instead of using fixed values  
783 for these parameters, for instance fixed  $\rho$  in the lag innovations or  $\sigma_\lambda^2$  in the inflation methods,  
784 we suggest using time-dependent adaptations. This adaptive solution could avoid the problems  
785 of instabilities close to the solution. Another option could be to adapt these procedures, working  
786 with stable parameter values (small  $\rho$ , low  $\sigma_\lambda^2$ ) and iterating the procedures on a batch of obser-  
787 vations, as in the EM algorithm. This offline variant was suggested and tested in Desroziers et al.  
788 (2005) with encouraging results. To the best of our knowledge, it has not yet been tested with  
789 lag-innovation methods.

790 The second challenge concerns considering time-varying error covariance matrices. The adap-  
791 tive procedures, based on online estimations with temporal smoothing of  $\mathbf{Q}$  and  $\mathbf{R}$ , are supposed  
792 to capture slowly evolving covariances. On the contrary, offline methods like the EM algorithm  
793 are working on a batch of observations, assuming that  $\mathbf{Q}$  and  $\mathbf{R}$  are constant over the batch period.  
794 Online solutions for the EM algorithm, with the likelihood averaged locally over time (Cocucci  
795 et al. 2020), could also capture slow evolution of the covariances. Another simple solution could  
796 be to work on small sets of observations, named as mini-batches, and to apply the EM algorithm  
797 in each set using the previous estimates as an initial guess. These intermediate schemes are of  
798 common use in machine learning.

799 A third challenge has to do with the assumption, used by all of the methods described herein, that  
800 observation and model errors are mutually independent. Nevertheless, as pointed out in Berry and  
801 Sauer (2018), observation and model error are often correlated in real data assimilation problems  
802 (e.g., for satellite retrieval of Earth observations that uses model outputs in the inversion process).  
803 Methods based on Bayesian inference can, in principle, exploit existing model-to-observation cor-  
804 relations by using a prior joint distribution (i.e., not two individual ones). The explicit taking into  
805 account of this correlation can then constrain the optimization procedure. This is not possible in  
806 the other approaches described in this review, at least not in their standard known formulations,  
807 and the presence of model-observation correlation can deteriorate their accuracy.

808 A fourth challenge is common to all the methods presented in this review. Iterative versions  
809 of the presented algorithms need initial values or distributions for  $\mathbf{R}$  and  $\mathbf{Q}$  (or  $\mathbf{B} = \mathbf{P}^f$  in the  
810 case of Desroziers). But, as mentioned in Waller et al. (2016) for the Desroziers diagnostics,  
811 there is no guarantee that the algorithms will converge to the optimal solution. Indeed, in such  
812 an optimization problem, there are possibly several local and non-optimal solutions. Suboptimal  
813 specifications of  $\mathbf{R}$ ,  $\mathbf{Q}$ , or  $\mathbf{B}$  in the initial DA cycle will affect the final estimation results. There  
814 are several solutions to avoid this convergence problem: initialize the covariance matrices using  
815 physical expertise, execute the iterative algorithms several times with different initial covariance  
816 matrices, or use stochastic perturbations in the optimization algorithms to avoid to be trapped in  
817 local solutions. These aspects of convergence and sensitivity to initial conditions have so far been  
818 poorly addressed. It is therefore necessary to check which method is robust operationally.

819 The last remaining challenge concerns the estimation of other statistical parameters of the state-  
820 space model given in Eqs. (1) and (2) and associated filters. Indeed, the initial conditions  $\mathbf{x}(0)$  and  
821  $\mathbf{P}(0)$  are crucial for certain satellite retrieval problems and have to be estimated. This is the case,  
822 for instance, when the time sequence of observations is short (i.e., shorter than the spinup time

823 of the filter with an uninformative prior) or when filtering and smoothing are repeated on various  
824 iterations, as in the EM algorithm. Estimation methods should also consider the estimation of sys-  
825 tematic or time-varying biases, the deterministic part of  $\eta$  and  $\epsilon$ . This was initially proposed by  
826 Dee et al. (1999a) and tested in Dee et al. (1999b) in the case of maximizing the innovation like-  
827 lihood, in Dee (2005) in a state augmentation formulation, and was adapted to a Bayesian update  
828 formulation in Liu et al. (2017) and in Berry and Harlim (2017). Recently, the joint estimation of  
829 bias and covariance error terms, for the treatment of brightness temperatures from the European  
830 geostationary satellite, has been successfully applied in Merchant et al. (2020).

### 831 *c. Perspectives for geophysical DA*

832 Beyond the aforementioned potential improvements in the existing techniques, specific research  
833 directions need to be taken by the data assimilation community. The main one concerns the real-  
834 ization of a comprehensive numerical evaluation of the different methods for the estimation of  $\mathbf{Q}$   
835 and  $\mathbf{R}$ , built on an agreed experimental framework and a consensus model. Such an effort would  
836 help to evaluate (i) the pros and cons of the different methods (including their capability to deal  
837 with high dimensionality, localization in ensemble methods, and their practical feasibility), (ii)  
838 their effects on different error statistics (RMSE, coverage probabilities, and other diagnostics),  
839 (iii) the potential combination of the various methods (especially those considering constant or  
840 adaptive covariances), and (iv) the capability to take into account other sources of error (due for  
841 instance to improper parameterizations, multiplicative errors, or forcing terms).

842 The use of a realistic DA problem, with a high-dimensional state-space and a limited and het-  
843 erogeneous observational coverage should be addressed in the future. In that realistic case, the  
844 observational information per degree of freedom will be significantly lower, and the estimates of  
845  $\mathbf{Q}$  and  $\mathbf{R}$  will deteriorate. Parametric versions of these error covariance matrices will therefore be

846 necessary. Among the parameters, some of them will control the variances, and will be different  
847 depending on the variable. Other parameters will control the spatial correlation lengths, that could  
848 be isotropic or anisotropic, depending on the region of interest and the considered variable. Cross-  
849 correlations between variables will also have to be considered. Consequently,  $\mathbf{Q}$  and  $\mathbf{R}$  will be  
850 block-matrices with as few parameters as possible.

851 A further challenge for future work is the evaluation of the feasibility of estimating non-additive,  
852 non-Gaussian, and time-correlated noises under the current estimation frameworks. In this way,  
853 the need for observational constraints for the stochastic perturbation methods in the NWP com-  
854 munity could be considered within the estimation framework discussed in this review.

855 *Acknowledgments.* This work has been carried out as part of the Copernicus Marine Environment  
856 Monitoring Service (CMEMS) 3DA project. CMEMS is implemented by Mercator Ocean in the  
857 framework of a delegation agreement with the European Union. This work was also partially  
858 supported by FOCUS Establishing Supercomputing Center of Excellence. CEREIA is a member of  
859 Institut Pierre Simon Laplace (IPSL). A. C. has been funded by the project REDDA (#250711) of  
860 the Norwegian Research Council. A. C. was also supported by the Natural Environment Research  
861 Council (Agreement PR140015 between NERC and the National Centre for Earth Observation).  
862 We thank Paul Platzer, a second-year PhD student, who helped to popularize the summary and  
863 the introduction, and John C. Wells, Gilles-Olivier Guégan and Aimée Johansen for their English  
864 grammar corrections. We also thank the five anonymous reviewers for their precious comments  
865 and ideas to improve this review paper. Finally, we are immensely grateful to Prof. David M.  
866 Schultz, Editor in Chief of the *Monthly Weather Review*, for his detailed advice and careful reading  
867 of the paper.

### Four main algorithms to jointly estimate Q and R in data assimilation

```

- initialize inflation factor (for instance  $\lambda(1) = 1$ );

for  $k$  in  $1:K$  do
  for  $i$  in  $1:N_e$  do
    - compute forecast  $\mathbf{x}_i^f(k)$  using Eq. (4a);
    - compute innovation  $\mathbf{d}_i(k)$  using Eq. (4b);
  end
  - compute empirical covariance  $\tilde{\mathbf{P}}^f(k)$  of the  $\mathbf{x}_i^f(k)$ ;
  - compute  $\mathbf{K}^f(k)$  using Eq. (4c) where  $\tilde{\mathbf{P}}^f(k)\mathcal{H}_k^T$  and  $\mathcal{H}_k\tilde{\mathbf{P}}^f(k)\mathcal{H}_k^T$  are inflated by
     $\lambda(k)$ ;
  for  $i$  in  $1:N_e$  do
    - compute analysis  $\mathbf{x}_i^a(k)$  using Eq. (4d);
  end
  - compute mean innovations  $\mathbf{d}^{o-f}(k)$  and  $\mathbf{d}^{o-a}(k)$  with  $\mathbf{d}_i^{o-f}(k) = \mathbf{y}(k) - \mathcal{H}_k(\mathbf{x}_i^f(k))$ 
    and  $\mathbf{d}_i^{o-a}(k) = \mathbf{y}(k) - \mathcal{H}_k(\mathbf{x}_i^a(k))$ ;
  - update  $\mathbf{R}(k)$  from Eq. (6b) using the cross-covariance between  $\mathbf{d}_i^{o-f}(k)$  and  $\mathbf{d}_i^{o-a}(k)$ ;
  - estimate  $\tilde{\lambda}(k)$  using Eq. (8) where  $\mathcal{H}_k\tilde{\mathbf{P}}^f(k)\mathcal{H}_k^T$  is inflated by  $\lambda(k)$ ;
  - update  $\lambda(k+1)$  using temporal smoother;
end

```

**Algorithm 1:** Adaptive algorithm for the EnKF (Miyoshi et al. 2013)

- initialize  $\mathbf{Q}(1)$  and  $\mathbf{R}(1)$ ;

**for**  $k$  in  $1:K$  **do**

**for**  $i$  in  $1:N_e$  **do**

- compute forecast  $\mathbf{x}_i^f(k)$  using Eq. (4a);
- compute innovation  $\mathbf{d}_i(k)$  using Eq. (4b);

**end**

    - compute  $\mathbf{K}^f(k)$  using Eq. (4c);

**for**  $i$  in  $1:N_e$  **do**

- compute analysis  $\mathbf{x}_i^a(k)$  using Eq. (4d);

**end**

    - apply Eq. (12a) to get  $\tilde{\mathbf{P}}(k)$  using linearizations of  $\mathbf{M}_k$  and  $\mathbf{H}_k$  given in Eqs. (5a) and (5b);

    - estimate  $\tilde{\mathbf{Q}}(k)$  using Eq. (12b);

    - estimate  $\tilde{\mathbf{R}}(k)$  using Eq. (12c);

    - update  $\mathbf{Q}(k+1)$  and  $\mathbf{R}(k+1)$  using temporal smoothers;

**end**

**Algorithm 2:** Adaptive algorithm for the EnKF (Berry and Sauer 2013)



- define a priori distributions for  $\boldsymbol{\theta}$  (shape parameters of  $\mathbf{Q}$  and  $\mathbf{R}$ );

**for**  $k$  in  $1:K$  **do**

**for**  $i$  in  $1:N_e$  **do**

- draw samples  $\boldsymbol{\theta}_i(k)$  from  $p(\boldsymbol{\theta}|\mathbf{y}(1:k-1))$ ;
- compute forecast  $\mathbf{x}_i^f(k)$  using Eq. (4a) with  $\boldsymbol{\theta}_i(k)$ ;
- compute innovation  $\mathbf{d}_i(k)$  using Eq. (4b) with  $\boldsymbol{\theta}_i(k)$ ;

**end**

    - compute  $\mathbf{K}^f(k)$  using Eq. (4c);

**for**  $i$  in  $1:N_e$  **do**

- compute analysis  $\mathbf{x}_i^a(k)$  using Eq. (4d);

**end**

    - approximate Gaussian likelihood of innovations  $p(\mathbf{y}(k)|\mathbf{y}(1:k-1), \boldsymbol{\theta}(k))$  using

    empirical mean  $\bar{\mathbf{d}}(k) = \frac{1}{N_e} \sum_{i=1}^{N_e} \mathbf{d}_i(k)$  and empirical covariance

$$\boldsymbol{\Sigma}(k) = \frac{1}{N_e-1} \sum_{i=1}^{N_e} (\mathbf{d}_i(k) - \bar{\mathbf{d}}(k)) (\mathbf{d}_i(k) - \bar{\mathbf{d}}(k))^T \text{ with } \mathbf{d}_i(k) = \mathbf{y}(k) - \mathcal{H}_k(\mathbf{x}_i^f(k));$$

    - update  $p(\boldsymbol{\theta}|\mathbf{y}(1:k))$  using Eq. (16);

**end**

**Algorithm 3:** Adaptive algorithm for the EnKF (Stroud et al. 2018)

**while**  $p(\mathbf{y}(1:K)|\boldsymbol{\theta}_{(n)}) - p(\mathbf{y}(1:K)|\boldsymbol{\theta}_{(n-1)}) > \varepsilon$  **do**

**for**  $k$  in  $1:K$  **do**

**for**  $i$  in  $1:N_e$  **do**

- compute forecast  $\mathbf{x}_i^f(k)$  using Eq. (4a);
- compute innovation  $\mathbf{d}_i(k)$  using Eq. (4b);

**end**

- compute  $\mathbf{K}^f(k)$  using Eq. (4c);

**for**  $i$  in  $1:N_e$  **do**

- compute analysis  $\mathbf{x}_i^a(k)$  using Eq. (4d);

**end**

**end**

**for**  $k$  in  $K:1$  **do**

- compute  $\mathbf{K}^s(k)$  using Eq. (4e);

**for**  $i$  in  $1:N_e$  **do**

- compute reanalysis  $\mathbf{x}_i^s(k)$  using Eq. (4f);

**end**

**end**

- increment  $n \leftarrow n + 1$ ;

- estimate  $\mathbf{Q}_{(n)}$  using Eq. (21a);

- estimate  $\mathbf{R}_{(n)}$  using Eq. (21b);

**end**

**Algorithm 4:** EM algorithm for the EnKF/EnKS (Dreano et al. 2017)

870 **References**

- 871 Anderson, J. L., 2007: An adaptive covariance inflation error correction algorithm for ensemble  
872 filters. *Tellus A: Dynamic Meteorology and Oceanography*, **59 (2)**, 210–224.
- 873 Anderson, J. L., 2009: Spatially and temporally varying adaptive covariance inflation for ensemble  
874 filters. *Tellus, Series A: Dynamic Meteorology and Oceanography*, **61 (1)**, 72–83.
- 875 Anderson, J. L., and S. L. Anderson, 1999: A Monte Carlo Implementation of the Nonlinear  
876 Filtering Problem to Produce Ensemble Assimilations and Forecasts. *Monthly Weather Review*,  
877 **12 (127)**, 2741–2758.
- 878 Bélanger, P. R., 1974: Estimation of noise covariance matrices for a linear time-varying stochastic  
879 process. *Automatica*, **10 (3)**, 267–275.
- 880 Berry, T., and J. Harlim, 2017: Correcting Biased Observation Model Error in Data Assimilation.  
881 *Monthly Weather Review*, **145 (7)**, 2833–2853.
- 882 Berry, T., and T. Sauer, 2013: Adaptive ensemble Kalman filtering of non-linear systems. *Tellus*,  
883 *Series A: Dynamic Meteorology and Oceanography*, **65 (20331)**, 1–16.
- 884 Berry, T., and T. Sauer, 2018: Correlation between system and observation errors in data assimila-  
885 tion. *Monthly Weather Review*, **146 (9)**, 2913–2931.
- 886 Bishop, C. H., and E. A. Satterfield, 2013: Hidden error variance theory. Part I: Exposition and  
887 analytic model. *Monthly Weather Review*, **141 (5)**, 1454–1468.
- 888 Bishop, C. H., E. A. Satterfield, and K. T. Shanley, 2013: Hidden error variance theory. Part  
889 II: An instrument that reveals hidden error variance distributions from ensemble forecasts and  
890 observations. *Monthly Weather Review*, **141 (5)**, 1469–1483.

- 891 Blanchet, I., C. Frankignoul, and M. A. Cane, 1997: A comparison of adaptive kalman filters for  
892 a tropical pacific ocean model. *Monthly Weather Review*, **125** (1), 40–58.
- 893 Bocquet, M., 2011: Ensemble Kalman filtering without the intrinsic need for inflation. *Nonlinear*  
894 *Processes in Geophysics*, **18** (5), 735–750.
- 895 Bocquet, M., P. N. Raanes, and A. Hannart, 2015: Expanding the validity of the ensemble Kalman  
896 filter without the intrinsic need for inflation. *Nonlinear Processes in Geophysics*, **22**, 645–662.
- 897 Bocquet, M., and P. Sakov, 2012: Combining inflation-free and iterative ensemble Kalman filters  
898 for strongly nonlinear systems. *Nonlinear Processes in Geophysics*, **19**, 383–399.
- 899 Bormann, N., A. Collard, and P. Bauer, 2010: Estimates of spatial and interchannel observation-  
900 error characteristics for current sounder radiances for numerical weather prediction. II: Applica-  
901 tion to AIRS and IASI data. *Quarterly Journal of the Royal Meteorological Society*, **136** (649),  
902 1051–1063.
- 903 Bowler, N. E., 2017: On the diagnosis of model error statistics using weak-constraint data assimi-  
904 lation. *Quarterly Journal of the Royal Meteorological Society*, **143** (705), 1916–1928.
- 905 Brankart, J.-M., E. Cosme, C.-E. Testut, P. Brasseur, and J. Verron, 2010: Efficient adaptive error  
906 parameterizations for square root or ensemble Kalman filters: Application to the control of  
907 ocean mesoscale signals. *Monthly Weather Review*, **138** (3), 932–950.
- 908 Buehner, M., 2010: Error statistics in data assimilation: Estimation and modelling. *Data Assimi-*  
909 *lation*, Springer, 93–112.
- 910 Campbell, W. F., E. A. Satterfield, B. Ruston, and N. L. Baker, 2017: Accounting for correlated ob-  
911 servation error in a dual-formulation 4D variational data assimilation system. *Monthly Weather*  
912 *Review*, **145** (3), 1019–1032.

- 913 Cappé, O., 2011: Online Expectation-Maximisation. *Mixtures: Estimation and Applications*, Wi-  
914 ley Series in Probability and Statistics, 1–53.
- 915 Carrassi, A., M. Bocquet, L. Bertino, and G. Evensen, 2018: Data Assimilation in the Geosciences:  
916 An overview on methods, issues and perspectives. *WIREs Clim Change*, **9 (5)**, e535.
- 917 Chapnik, B., G. Desroziers, F. Rabier, and O. Talagrand, 2004: Properties and first application  
918 of an error-statistics tuning method in variational assimilation. *Quarterly Journal of the Royal*  
919 *Meteorological Society*, **130 (601)**, 2253–2275.
- 920 Cocucci, T. J., M. Pulido, M. Lucini, and P. Tandeo, 2020: Model error covariance estimation  
921 in particle and ensemble Kalman filters using an online expectation-maximization algorithm.  
922 *arXiv preprint arXiv:2003.02109*.
- 923 Corazza, M., E. Kalnay, D. J. Patil, R. Morss, M. Cai, I. Szunyogh, B. R. Hunt, and J. A. Yorke,  
924 2003: Use of the breeding technique to estimate the structure of the analysis “errors of the day”.  
925 *Nonlinear Processes in Geophysics*, **10 (3)**, 233–243.
- 926 Daescu, D. N., and R. H. Langland, 2013: Error covariance sensitivity and impact estimation with  
927 adjoint 4D-Var: theoretical aspects and first applications to NAVDAS-AR. *Quarterly Journal of*  
928 *the Royal Meteorological Society*, **139**, 226–241.
- 929 Daescu, D. N., and R. Todling, 2010: Adjoint sensitivity of the model forecast to data assimilation  
930 system error covariance parameters. *Quarterly Journal of the Royal Meteorological Society*,  
931 **136**, 2000–2012.
- 932 Daley, R., 1991: Atmospheric data analysis. Cambridge University Press, 457 pp.
- 933 Daley, R., 1992: Estimating Model-Error Covariances for Application to Atmospheric Data As-  
934 simulation. *Monthly Weather Review*, **120 (8)**, 1735–1746.

- 935 Dee, D. P., 1995: On-line estimation of error covariance parameters for atmospheric data assimi-  
936 lation. *Monthly Weather Review*, **123** (4), 1128–1145.
- 937 Dee, D. P., 2005: Bias and data assimilation. *Quarterly Journal of the Royal Meteorological Soci-*  
938 *ety*, **131** (613), 3323–3343.
- 939 Dee, D. P., S. E. Cohn, A. Dalcher, and M. Ghil, 1985: An efficient algorithm for estimating  
940 noise covariances in distributed systems. *IEEE Transactions on Automatic Control*, **30** (11),  
941 1057–1065.
- 942 Dee, D. P., G. Gaspari, C. Redder, L. Rukhovets, and A. M. da Silva, 1999a: Maximum-  
943 likelihood estimation of forecast and observation error covariance parameters. Part I: Method-  
944 ology. *Monthly Weather Review*, **127** (1992), 1822–1834.
- 945 Dee, D. P., G. Gaspari, C. Redder, L. Rukhovets, and A. M. da Silva, 1999b: Maximum-  
946 likelihood estimation of forecast and observation error covariance parameters. Part II: Appli-  
947 cations. *Monthly Weather Review*, **127** (1992), 1835–1849.
- 948 Delsole, T., and X. Yang, 2010: State and parameter estimation in stochastic dynamical models.  
949 *Physica D: Nonlinear Phenomena*, **239** (18), 1781–1788.
- 950 Dempster, A. P., N. M. Laird, and D. B. Rubin, 1977: Maximum Likelihood from Incomplete  
951 Data via the EM Algorithm. *Journal of the Royal Statistical Society. Series B (Methodological)*,  
952 **39** (1), 1–38.
- 953 Desroziers, G., L. Berre, B. Chapnik, and P. Poli, 2005: Diagnosis of observation, background and  
954 analysis-error statistics in observation space. *Quarterly Journal of the Royal Meteorological*  
955 *Society*, **131** (613), 3385–3396.

- 956 Desroziers, G., and S. Ivanov, 2001: Diagnosis and adaptive tuning of observation-error pa-  
957 rameters in a variational assimilation. *Quarterly Journal of the Royal Meteorological Society*,  
958 **127 (574)**, 1433–1452.
- 959 Dreano, D., P. Tandeo, M. Pulido, T. Chonavel, B. Ait-El-Fquih, and I. Hoteit, 2017: Estimat-  
960 ing model error covariances in nonlinear state-space models using Kalman smoothing and the  
961 expectation-maximisation algorithm. *Quarterly Journal of the Royal Meteorological Society*,  
962 **143 (705)**, 1877–1885.
- 963 Duník, J., O. Straka, O. Kost, and J. Havlík, 2017: Noise covariance matrices in state-space mod-  
964 els: A survey and comparison of estimation methods-Part I. *International Journal of Adaptive*  
965 *Control and Signal Processing*, **31 (11)**, 1505–1543.
- 966 El Gharamti, M., 2018: Enhanced Adaptive Inflation Algorithm for Ensemble Filters. *Monthly*  
967 *Weather Review*, **146**, 623–640.
- 968 Evensen, G., 2009: *Data assimilation: the ensemble Kalman filter*. Springer Science & Business  
969 Media.
- 970 Frei, M., and H. R. Künsch, 2012: Sequential State and Observation Noise Covariance Estimation  
971 Using Combined Ensemble Kalman and Particle Filters. *Monthly Weather Review*, **140 (5)**,  
972 1476–1495.
- 973 Fu, L.-L., I. Fukumori, and R. N. Miller, 1993: Fitting dynamic models to the Geosat sea level ob-  
974 servations in the tropical Pacific ocean. Part II: A linear, wind-driven model. *Journal of Physical*  
975 *Oceanography*, **23 (10)**, 2162–2181.
- 976 Ghil, M., and P. Malanotte-Rizzoli, 1991: Data assimilation in meteorology and oceanography.pdf.  
977 *Advances in Geophysics*, **33**, 141–266.

- 978 Guillet, O., A. T. Weaver, X. Vasseur, Y. Michel, S. Gratton, and S. Gürol, 2019: Modelling  
979 spatially correlated observation errors in variational data assimilation using a diffusion operator  
980 on an unstructured mesh. *Quarterly Journal of the Royal Meteorological Society*, doi:10.1002/  
981 qj.3537.
- 982 Harlim, J., 2018: Ensemble Kalman Filters. *Data-Driven Computational Methods*, Cambridge  
983 university press, 31–59.
- 984 Harlim, J., A. Mahdi, and A. J. Majda, 2014: An ensemble Kalman filter for statistical estimation  
985 of physics constrained nonlinear regression models. *Journal of Computational Physics*, **257**,  
986 782–812.
- 987 Hollingsworth, A., and P. Lönnberg, 1986: The statistical structure of short-range forecast errors  
988 as determined from radiosonde data. Part I: The wind field. *Tellus A*, **38 (2)**, 111–136.
- 989 Hotta, D., E. Kalnay, Y. Ota, and T. Miyoshi, 2017: EFSR: Ensemble forecast sensitivity to obser-  
990 vation error covariance. *Monthly Weather Review*, **145**, 5015–5031.
- 991 Houtekamer, P. L., H. L. Mitchell, and X. Deng, 2009: Model Error Representation in an Opera-  
992 tional Ensemble Kalman Filter. *Monthly Weather Review*, **137 (7)**, 2126–2143.
- 993 Houtekamer, P. L., and F. Zhang, 2016: Review of the Ensemble Kalman Filter for Atmospheric  
994 Data Assimilation. *Monthly Weather Review*, **144 (12)**, 4489–4532.
- 995 Ide, K., P. Courtier, M. Ghil, and A. C. Lorenc, 1997: Unified Notation for Data Assimilation:  
996 Operational, Sequential and Variational. *Journal of the Meteorological Society of Japan*, **75 (1)**,  
997 181–189.
- 998 Janjić, T., and Coauthors, 2018: On the representation error in data assimilation. *Quarterly Journal*  
999 *of the Royal Meteorological Society*, **144 (713)**, 1257–1278.



- 1000 Jazwinski, A. H., 1970: *Stochastic processes and filtering theory*. Academic Press.
- 1001 Kantas, N., A. Doucet, S. S. Singh, J. Maciejowski, and N. Chopin, 2015: On particle methods for  
1002 parameter estimation in state-space models. *Statistical Science*, **30** (3), 328–351.
- 1003 Katzfuss, M., J. R. Stroud, and C. K. Wikle, 2019: Ensemble Kalman methods for high-  
1004 dimensional hierarchical dynamic space-time models. *Journal of the American Statistical Asso-  
1005 ciation*, 1–43.
- 1006 Kotsuki, S., T. Miyoshi, K. Terasaki, G.-Y. Lien, and E. Kalnay, 2017a: Assimilating the global  
1007 satellite mapping of precipitation data with the Nonhydrostatic Icosahedral Atmospheric Model  
1008 (NICAM). *Journal of Geophysical Research: Atmospheres*, **122** (2), 631–650.
- 1009 Kotsuki, S., Y. Ota, and T. Miyoshi, 2017b: Adaptive covariance relaxation methods for ensemble  
1010 data assimilation: Experiments in the real atmosphere. *Quarterly Journal of the Royal Meteoro-  
1011 logical Society*, **143** (705), 2001–2015.
- 1012 Leith, C. E., 1978: Objective methods for weather prediction. *Annual Review of Fluid Mechanics*,  
1013 **10** (1), 107–128.
- 1014 Li, H., E. Kalnay, and T. Miyoshi, 2009: Simultaneous estimation of covariance inflation and  
1015 observation errors within an ensemble Kalman filter. *Quarterly Journal of the Royal Meteoro-  
1016 logical Society*, **135** (2), 523–533.
- 1017 Liang, X., X. Zheng, S. Zhang, G. Wu, Y. Dai, and Y. Li, 2012: Maximum likelihood estimation of  
1018 inflation factors on error covariance matrices for ensemble Kalman filter assimilation. *Quarterly  
1019 Journal of the Royal Meteorological Society*, **138** (662), 263–273.
- 1020 Liu, J., and M. West, 2001: Combined parameter and state estimation in simulation-based filtering.  
1021 *Sequential Monte Carlo methods in practice*, Springer, 197–223.

- 1022 Liu, Y., J.-M. Haussaire, M. Bocquet, Y. Roustan, O. Saunier, and A. Mathieu, 2017: Uncertainty  
1023 quantification of pollutant source retrieval: comparison of Bayesian methods with application to  
1024 the Chernobyl and Fukushima Daiichi accidental releases of radionuclides. *Quarterly Journal*  
1025 *of the Royal Meteorological Society*, **143 (708)**, 2886–2901.
- 1026 Mehra, R. K., 1970: On the identification of variances and adaptive Kalman filtering. *IEEE Trans-*  
1027 *actions on Automatic Control*, **AC-15 (2)**, 175–184.
- 1028 Mehra, R. K., 1972: Approaches to adaptive filtering. *IEEE Transactions on Automatic Control*,  
1029 **17 (5)**, 693–698.
- 1030 Ménard, R., 2016: Error covariance estimation methods based on analysis residuals: theoretical  
1031 foundation and convergence properties derived from simplified observation networks. *Quarterly*  
1032 *Journal of the Royal Meteorological Society*, **142 (694)**, 257–273.
- 1033 Menemenlis, D., and M. Chechelnitsky, 2000: Error estimates for an ocean general circulation  
1034 model from altimeter and acoustic tomography data. *Monthly Weather Review*, **128 (3)**, 763–  
1035 778.
- 1036 Ménétrier, B., and T. Auligné, 2015: Optimized localization and hybridization to filter ensemble-  
1037 based covariances. *Monthly Weather Review*, **143**, 3931–3947.
- 1038 Merchant, C. J., S. Saux-Picart, and J. Waller, 2020: Bias correction and covariance parameters for  
1039 optimal estimation by exploiting matched in-situ references. *Remote Sensing of Environment*,  
1040 **237**, 111 590.
- 1041 Mitchell, H. L., and P. L. Houtekamer, 2000: An adaptive ensemble Kalman filter. *Monthly*  
1042 *Weather Review*, **128 (2)**, 416–433.

- 1043 Mitchell, L., and A. Carrassi, 2015: Accounting for model error due to unresolved scales within  
1044 ensemble Kalman filtering. *Quarterly Journal of the Royal Meteorological Society*, **141 (689)**,  
1045 1417–1428.
- 1046 Miyoshi, T., 2011: The Gaussian Approach to Adaptive Covariance Inflation and Its Implemen-  
1047 tation with the Local Ensemble Transform Kalman Filter. *Monthly Weather Review*, **139 (5)**,  
1048 1519–1535.
- 1049 Miyoshi, T., E. Kalnay, and H. Li, 2013: Estimating and including observation-error correlations  
1050 in data assimilation. *Inverse Problems in Science and Engineering*, **21 (3)**, 387–398.
- 1051 Miyoshi, T., Y. Sato, and T. Kadowaki, 2010: Ensemble Kalman filter and 4D-Var intercomparison  
1052 with the Japanese operational global analysis and prediction system. *Monthly Weather Review*,  
1053 **138 (7)**, 2846–2866.
- 1054 Pham, D. T., J. Verron, and M. C. Roubaud, 1998: A singular evolutive extended Kalman filter for  
1055 data assimilation in oceanography. *Journal of Marine systems*, **16 (3-4)**, 323–340.
- 1056 Pulido, M., P. Tandeo, M. Bocquet, A. Carrassi, and M. Lucini, 2018: Stochastic parameterization  
1057 identification using ensemble Kalman filtering combined with maximum likelihood methods.  
1058 *Tellus A: Dynamic Meteorology and Oceanography*, **70 (1)**, 1442 099.
- 1059 Purser, R. J., and D. F. Parrish, 2003: A Bayesian technique for estimating continuously varying  
1060 statistical parameters of a variational assimilation. *Meteorology and Atmospheric Physics*, **82 (1-**  
1061 **4)**, 209–226.
- 1062 Raanes, P. N., M. Bocquet, and A. Carrassi, 2019: Adaptive covariance inflation in the ensem-  
1063 ble Kalman filter by Gaussian scale mixtures. *Quarterly Journal of the Royal Meteorological*  
1064 *Society*, **145 (718)**, 53–75.

- 1065 Rodwell, M. J., and T. N. Palmer, 2007: Using numerical weather prediction to assess climate  
1066 models. *Quarterly Journal of the Royal Meteorological Society*, **133** (622), 129–146.
- 1067 Ruiz, J. J., M. Pulido, and T. Miyoshi, 2013a: Estimating model parameters with ensemble-based  
1068 data assimilation: A review. *Journal of the Meteorological Society of Japan*, **91**, 79–99.
- 1069 Ruiz, J. J., M. Pulido, and T. Miyoshi, 2013b: Estimating model parameters with ensemble-based  
1070 data assimilation: Parameter Covariance Treatment. *Journal of the Meteorological Society of*  
1071 *Japan*, **91**, 453–469.
- 1072 Rutherford, I. D., 1972: Data assimilation by statistical interpolation of forecast error fields. *Jour-*  
1073 *nal of the Atmospheric Sciences*, **29** (5), 809–815.
- 1074 Satterfield, E. A., D. Hodyss, D. D. Kuhl, and C. H. Bishop, 2018: Observation-informed gener-  
1075 alized hybrid error covariance models. *Monthly Weather Review*, **146**, 3605–3622.
- 1076 Scheffler, G., J. Ruiz, and M. Pulido, 2019: Inference of stochastic parametrizations for model  
1077 error treatment using nested ensemble Kalman filters. *Quarterly Journal of the Royal Meteoro-*  
1078 *logical Society*, doi:<https://doi.org/10.1002/qj.3542>.
- 1079 Schmidt, S. F., 1966: Applications of state space methods to navigation problems. *Advances in*  
1080 *Control Systems*, **3**, 293–340.
- 1081 Shumway, R. H., and D. S. Stoffer, 1982: An approach to time series smoothing and forecasting  
1082 using the EM algorithm. *Journal of Time Series Analysis*, **3** (4), 253–264.
- 1083 Solonen, A., J. Hakkarainen, A. Ilin, M. Abbas, and A. Bibov, 2014: Estimating model error  
1084 covariance matrix parameters in extended Kalman filtering. *Nonlinear Processes in Geophysics*,  
1085 **21** (5), 919–927.

- 1086 Stroud, J. R., and T. Bengtsson, 2007: Sequential state and variance estimation within the ensemble  
1087 Kalman filter. *Monthly Weather Review*, **135** (9), 3194–3208.
- 1088 Stroud, J. R., M. Katzfuss, and C. K. Wikle, 2018: A Bayesian adaptive ensemble Kalman filter  
1089 for sequential state and parameter estimation. *Monthly Weather Review*, **146** (1), 373–386.
- 1090 Tandeo, P., M. Pulido, and F. Lott, 2015: Offline parameter estimation using EnKF and maximum  
1091 likelihood error covariance estimates: Application to a subgrid-scale orography parametrization.  
1092 *Quarterly Journal of the Royal Meteorological Society*, **141** (687), 383–395.
- 1093 Todling, R., 2015: A lag-1 smoother approach to system-error estimation: sequential method.  
1094 *Quarterly Journal of the Royal Meteorological Society*, **141** (690), 1502–1513.
- 1095 Ueno, G., T. Higuchi, T. Kagimoto, and N. Hirose, 2010: Maximum likelihood estimation of error  
1096 covariances in ensemble-based filters and its application to a coupled atmosphere-ocean model.  
1097 *Quarterly Journal of the Royal Meteorological Society*, **136** (650), 1316–1343.
- 1098 Ueno, G., and N. Nakamura, 2014: Iterative algorithm for maximum-likelihood estimation of the  
1099 observation-error covariance matrix for ensemble-based filters. *Quarterly Journal of the Royal  
1100 Meteorological Society*, **140** (678), 295–315.
- 1101 Ueno, G., and N. Nakamura, 2016: Bayesian estimation of the observation-error covariance matrix  
1102 in ensemble-based filters. *Quarterly Journal of the Royal Meteorological Society*, **142** (698),  
1103 2055–2080.
- 1104 Wahba, G., and J. Wendelberger, 1980: Some new mathematical methods for variational objective  
1105 analysis using splines and cross validation. *Monthly weather review*, **108** (8), 1122–1143.

- 1106 Waller, J. A., S. L. Dance, and N. K. Nichols, 2016: Theoretical insight into diagnosing obser-  
1107 vation error correlations using observation-minus-background and observation-minus-analysis  
1108 statistics. *Quarterly Journal of the Royal Meteorological Society*, **142 (694)**, 418–431.
- 1109 Waller, J. A., S. L. Dance, and N. K. Nichols, 2017: On diagnosing observation-error statistics  
1110 with local ensemble data assimilation. *Quarterly Journal of the Royal Meteorological Society*,  
1111 **143 (708)**, 2677–2686.
- 1112 Wang, X., and C. H. Bishop, 2003: A Comparison of Breeding and Ensemble Transform Kalman  
1113 Filter Ensemble Forecast Schemes. *Journal of the Atmospheric Sciences*, **60 (9)**, 1140–1158.
- 1114 Weston, P. P., W. Bell, and J. R. Eyre, 2014: Accounting for correlated error in the assimilation of  
1115 high-resolution sounder data. *Quarterly Journal of the Royal Meteorological Society*, **140 (685)**,  
1116 2420–2429.
- 1117 Whitaker, J. S., and T. M. Hamill, 2012: Evaluating methods to account for system errors in  
1118 ensemble data assimilation. *Monthly Weather Review*, **140 (9)**, 3078–3089.
- 1119 Whitaker, J. S., T. M. Hamill, X. Wei, Y. Song, and Z. Toth, 2008: Ensemble data assimilation  
1120 with the NCEP global forecast system. *Monthly Weather Review*, **136 (2)**, 463–482.
- 1121 Winiarek, V., M. Bocquet, N. Duhanyan, Y. Roustan, O. Saunier, and A. Mathieu, 2014: Esti-  
1122 mation of the caesium-137 source term from the Fukushima Daiichi nuclear power plant using  
1123 a consistent joint assimilation of air concentration and deposition observations. *Atmospheric*  
1124 *Environment*, **82**, 268–279.
- 1125 Winiarek, V., M. Bocquet, O. Saunier, and A. Mathieu, 2012: Estimation of errors in the inverse  
1126 modeling of accidental release of atmospheric pollutant: Application to the reconstruction of

- 1127 the cesium-137 and iodine-131 source terms from the Fukushima Daiichi power plant. *Journal*  
1128 *of Geophysical Research: Atmospheres*, **117 (D5)**.
- 1129 Wu, C. F. J., 1983: On the convergence properties of the EM algorithm. *Annals of Statistics*, **11 (1)**,  
1130 95–103.
- 1131 Yang, Y., and E. Mémin, 2019: Estimation of physical parameters under location uncertainty using  
1132 an ensemble-expectation-maximization algorithm. *Quarterly Journal of the Royal Meteorolog-*  
1133 *ical Society*, **145 (719)**, 418–433.
- 1134 Ying, Y., and F. Zhang, 2015: An adaptive covariance relaxation method for ensemble data assim-  
1135 ilation. *Quarterly Journal of the Royal Meteorological Society*, **141 (692)**, 2898–2906.
- 1136 Zebiak, S. E., and M. A. Cane, 1987: A model El Niño–southern oscillation. *Monthly Weather*  
1137 *Review*, **115 (10)**, 2262–2278.
- 1138 Zhang, F., C. Snyder, and J. Sun, 2004: Impacts of initial estimate and observation availability on  
1139 convective-scale data assimilation with an ensemble Kalman filter. *Monthly Weather Review*,  
1140 **132 (5)**, 1238–1253.
- 1141 Zhen, Y., and J. Harlim, 2015: Adaptive error covariances estimation methods for ensemble  
1142 Kalman filters. *Journal of Computational Physics*, **294**, 619–638.

1143 **LIST OF TABLES**

1144 **Table 1.** Comparison of several methods to estimate error covariance matrices **Q** and **R**  
1145 in data assimilation. . . . . 63



TABLE 1. Comparison of several methods to estimate error covariance matrices  $\mathbf{Q}$  and  $\mathbf{R}$  in data assimilation.

Estimation method	Criteria	Estimation of covariance $\mathbf{Q}$	Suitable for non-Gaussian errors	Application to the highest complexity model
Method of moments	Innovation statistics in the observation space	No (inflation of $\mathbf{P}^f$ instead)	No	NWP
Method of moments	Lag innovation between consecutive times	Yes	No	Lorenz-96
Likelihood methods	Bayesian update of the posterior distribution	No (or joint parameter with $\mathbf{R}$ )	Yes (using particle filters, not EnKF)	Shallow water
Likelihood methods	Maximization of the total likelihood	Yes	Yes (using particle filters, not EnKF)	Two-scale Lorenz-96

1146

## LIST OF FIGURES

1147

**Fig. 1.** Sketch of sequential and ensemble data assimilation algorithms in the observation space (i.e., in the space of the observations  $\mathbf{y}$ ), where the observation operator  $\mathcal{H}$  is omitted for simplicity. The ellipses represent the forecast  $\mathbf{P}^f$  and analysis  $\mathbf{P}^a$  error covariances, while the model  $\mathbf{Q}$  and observation  $\mathbf{R}$  error covariances are the unknown entries of the state-space model in Eqs. (1) and (2). The forecast error covariance matrix is written  $\mathbf{P}^f$  and is the sum of  $\mathbf{P}^m$ , the forecasted state  $\mathbf{x}^f$  spread, and the model error  $\mathbf{Q}$ . This scheme is a modified version based on Fig. 1 from Carrassi et al. (2018). . . . . 65

1148

1149

1150

1151

1152

1153

1154

**Fig. 2.** Example of a univariate AR(1) process generated using Eq. (3) with  $Q^t = 1$  (red line), noisy observations as in Eq. (2) with  $R^t = 1$  (black dots) and reconstructions with a Kalman smoother (black lines and gray 95% confidence interval) with different values of  $Q$  and  $R$ , from 0.1 to 10. The optimal values of RMSE and coverage probabilities are, respectively, 0.71 and 95%. . . . . 66

1155

1156

1157

1158

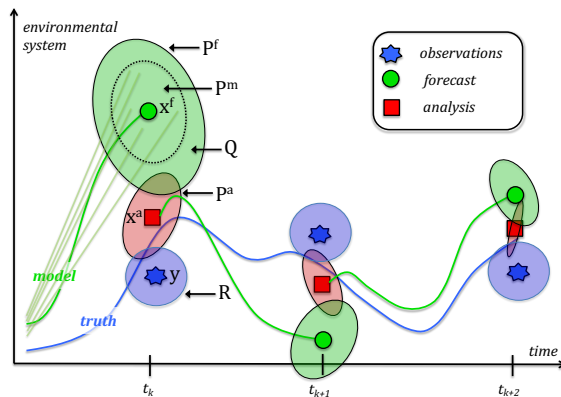
1159

**Fig. 3.** Timeline of the main methods used in geophysical data assimilation for the joint estimation of  $\mathbf{Q}$  and  $\mathbf{R}$  over the last 15 years. Dee (1995) and Desroziers and Ivanov (2001) are not represented here but are certainly the seminal work of this research field in data assimilation. . . . . 67

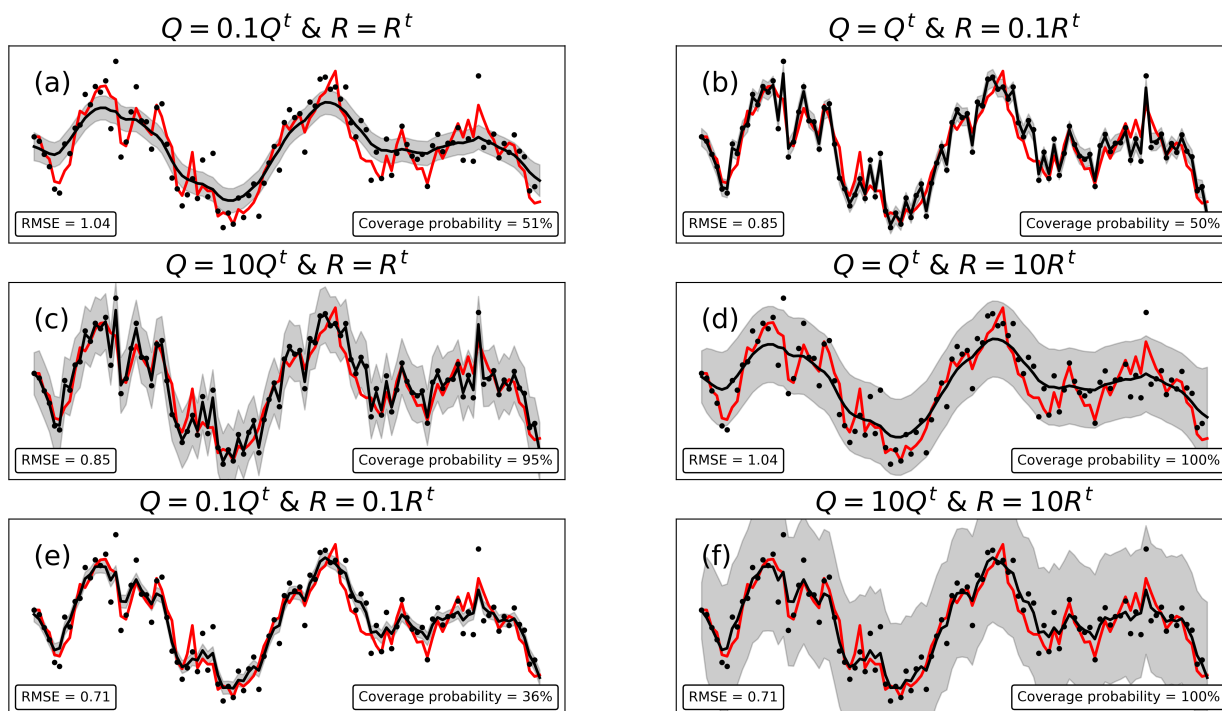
1160

1161

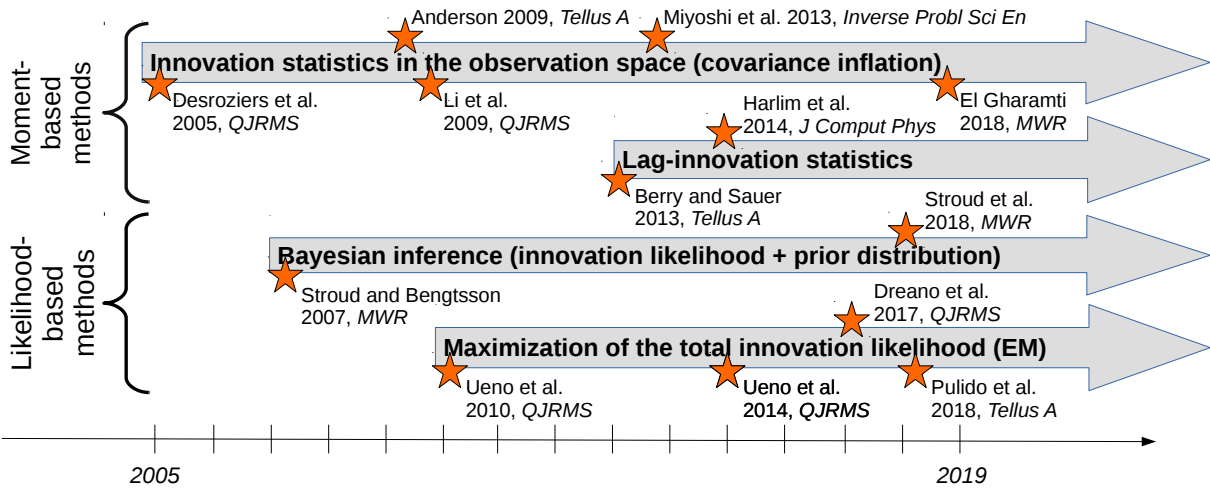
Downloaded from <http://journals.ametsoc.org/mwr/article-pdf/doi/10.1175/MWR-D-19-0240.1/4992874/mwr190240.pdf> by guest on 26 August 2020



1162 FIG. 1. Sketch of sequential and ensemble data assimilation algorithms in the observation space (i.e., in the  
 1163 space of the observations  $\mathbf{y}$ ), where the observation operator  $\mathcal{H}$  is omitted for simplicity. The ellipses represent  
 1164 the forecast  $\mathbf{P}^f$  and analysis  $\mathbf{P}^a$  error covariances, while the model  $\mathbf{Q}$  and observation  $\mathbf{R}$  error covariances are the  
 1165 unknown entries of the state-space model in Eqs. (1) and (2). The forecast error covariance matrix is written  $\mathbf{P}^f$   
 1166 and is the sum of  $\mathbf{P}^m$ , the forecasted state  $\mathbf{x}^f$  spread, and the model error  $\mathbf{Q}$ . This scheme is a modified version  
 1167 based on Fig. 1 from Carrassi et al. (2018).



1168 FIG. 2. Example of a univariate AR(1) process generated using Eq. (3) with  $Q^t = 1$  (red line), noisy observa-  
 1169 tions as in Eq. (2) with  $R^t = 1$  (black dots) and reconstructions with a Kalman smoother (black lines and gray  
 1170 95% confidence interval) with different values of  $Q$  and  $R$ , from 0.1 to 10. The optimal values of RMSE and  
 1171 coverage probabilities are, respectively, 0.71 and 95%.



1172 FIG. 3. Timeline of the main methods used in geophysical data assimilation for the joint estimation of  $\mathbf{Q}$  and  
 1173  $\mathbf{R}$  over the last 15 years. Dee (1995) and Desroziers and Ivanov (2001) are not represented here but are certainly  
 1174 the seminal work of this research field in data assimilation.